Small Cationic Antimicrobial Peptides Delocalize Peripheral Membrane Proteins

Michaela Wenzel[a], Alina Iulia Chiriac[b], Andreas Otto[c], Dagmar Zweytick[d], Caroline May[e], Catherine Schumacher[f], Ronald Gust[g], H. Bauke Albada[h], Maya Penkova[h], Ute Krämer[i], Ralf Erdmann[j], Nils Metzler-Nolte[h], Suzana K. Straus[k], Erhard Bremer[l], Dörte Becher[c], Heike Brötz-Oesterhelt[f], Hans-Georg Sahl[b], Julia E. Bandow[a1]

[a]*Biology of Microorganisms, Ruhr University Bochum, Bochum, Germany*
[b]*Institute for Medical Microbiology, Immunology, and Parasitology, Pharmaceutical Microbiology Section, University of Bonn, Bonn, Germany*
[c]*Microbial Physiology and Molecular Biology, Ernst Moritz Arndt University, Greifswald, Germany*
[d]*Institute of Molecular Biosciences, Biophysics Division, University of Graz, Graz, Austria*
[e]*Immune Proteomics, Medical Proteome Center, Ruhr University Bochum, Bochum, Germany*
[f]*Institute for Pharmaceutical Biology and Biotechnology, Heinrich Heine University, Düsseldorf, Germany*
[g]*Department of Pharmaceutical Chemistry, University of Innsbruck, Austria*
[h]*Bioinorganic Chemistry, Ruhr University Bochum, Bochum, Germany*
[i]*Plant Physiology, Ruhr University Bochum, Bochum, Germany*
[j]*Institute of Physiological Chemistry, Ruhr University Bochum, Bochum, Germany*
[k]*Department of Chemistry, University of British Columbia, Vancouver, Canada*
[l]*Department of Biology, University of Marburg, Marburg, Germany*

SI Appendix

Content

i) Experimental details

Antibiotics

Antibiotic stock solutions of 10 mg/ml were prepared in sterile DMSO (MP196, D-MP196, MP276, valinomycin, gramicidin A, gramicidin S, vancomycin), sterile double-distilled water (aurein 2.2), or 0.01 M HCl (nisin). MP276, L- and D-MP196 were synthesized by solid-phase synthesis as described previously (1) (see **SI Appendix, Fig. S1** for structures). Nisin was purified according to Bonelli *et al*. (2). Valinomycin, gramicidin A, and vancomycin were purchased from Sigma-Aldrich (St Louis, MO, USA). Gramicidin S was synthesized according to Wadwhani *et al*. (3). Aurein 2.2 was synthesized as described by Pan *et al.* (4). Lactoferrin, rotenone, and antimycin A were purchased from Sigma-Aldrich. Stock solutions were prepared in sterile double-distilled water (lactoferrin, 1 mM), acetone (rotenone, 100 mM), or ethanol (antimycin A, 10 mM). Sublethal antibiotic concentrations applied in the single experiments were adjusted to the respective bacterial strains and experimental conditions, aiming at adequate bacterial growth inhibition (reduction of the growth rate by 50-70%) without killing the cells or abolishing their metabolic activity completely (see **SI Appendix, Fig. S2**).

Radioactive precursor incorporation assay

Influence of MP196 on major metabolic pathways was studied by incorporation of radioactively labeled precursor molecules into *Staphylococcus simulans* 22 as described by Schneider *et al.* (5). (^{14}C)-thymidine was used for monitoring DNA, 5-(^{3}H)-uridine for RNA, L-(^{14}C)-isoleucine for protein, and (^{3}H)-glucosamine-hydrochloride for cell wall biosynthesis inhibition, respectively. Cells were grown in half-concentrated Mueller Hinton broth (Henceforth MH, Oxoid, Basingstoke, United Kingdom) at 37 °C until reaching an optical density at 600 nm (OD_{600}) of 0.5 and diluted to an OD_{600} of 0.1 to 0.2. Newly synthesized DNA, RNA, protein or peptidoglycane was radioactively labeled by addition of the respective precursors to a final concentration of 5.55 kBq/mL (^{14}C)-thymidine, 37 kBq/mL 5-(^{3}H)-uridine, 5.55 kBq/mL L-(^{14}C)-isoleucine, and 37 kBq/mL (^{3}H)-glucosamine-hydrochloride. After 15 ((^{14}C)-thymidine, 5-(^{3}H)-uridine, L-(^{14}C)-isoleucine) or 30 min ((^{3}H)-glucosamine-hydrochloride) of radioactive incorporation, subcultures of the differentially labeled samples were treated with 2 µg/ml MP196, 0.7

µg/ml ciprofloxacin, 0.07 µg/ml rifampicin, 0.7 µg/ml tetracycline, and 0.7 µg/ml vancomycin, respectively, or left untreated as negative controls. Samples of 200 µl were collected at 0, 10, 20, and 30 min after antibiotic addition, mixed with ice-cold trichloroacetic acid (TCA) precipitation buffer (10% TCA, 1 M NaCl), incubated on ice for 30 min, and filtered through glass microfibre filters (Whatman, GE Healthcare, Uppsala, Sweden). Filters were subsequently washed with 5 ml washing buffer (2.5% TCA, 1 M NaCl), dried, and transferred to counting vials. 5 ml of scintillation fluid (Filtersafe, Zinsser, Frankfurt, Germany) were added and radioactivity was measured in counts per minute (CPM) using a TriCarb 3110TR liquid scintillation analyzer (Perkin Elmer, Waltham, MA, USA).

Reporter gene assay

For quantitative expression analysis of selected marker genes, five bacterial reporter strains were used, carrying the promoter of either *yorB*, *bmrC* (synonym *yheI)*, *helD* (synonym *yvgS)*, *ypuA* or *liaI* (synonym *yvqI*) fused to the firefly luciferase reporter gene in the genetic background of *B. subtilis* IS34 (6). Reporter strains were cultured overnight in lysogeny broth with 5 µg/ml erythromycin (resistance marker on the luciferase plasmid) at 37 °C and 200 rpm. Cultures were diluted to OD_{600} of 0.05 in 20 ml of either Belitzky minimal medium (BMM) (7) (*bmrC* strain) or lysogeny broth (all other strains) with 5 µg/ml erythromycin, grown to an OD_{600} of 0.4 (*bmrC* strain) or 0.9 (all other strains) and diluted to an OD_{600} of 0.02. Serial twofold dilutions of MP196 (0.031 to 64 µg/ml) in 60 µl lysogeny broth or BMM were prepared in white 96-well flat bottom polystyrol microtiter plates (Greiner, Frickenhusen, Germany) and were inoculated with 60 µl of the adjusted bacterial suspension. Plates were incubated at 37 °C for a predetermined time period depending on the induction kinetics of the reporter strain: 1 h for the *liaI* and *ypuA* strains, 1.5 h for the *helD* strain, 3.5 h for the *yorB* strain and 4 h for the *bmrC* strain. Then 60 µl citrate buffer (0.1 M, pH 5) containing 2 mM luciferin (Serva, Heidelberg, Germany) was added and flash luminescence was measured using a microtiter plate reader (infinite M200, Tecan, Männedorf, Switzerland).

Proteome analysis

Bacterial strains and growth conditions

Bacillus subtilis 168 (*trpC2*) (8) was grown at 37 °C under steady agitation in BMM. Minimal inhibitory concentrations (MICs) were determined under proteomics conditions as described previously (9). In short, two ml of antibiotic-supplemented BMM were inoculated with $5x10^5$ bacteria per ml and incubated at 37 °C under steady agitation for 18 h. The MIC was defined as the lowest antibiotic concentration inhibiting visible growth. In growth experiments, bacterial cultures were treated with different MIC-based antibiotic concentrations after growing to an OD_{500} of 0.35. For proteomic experiments those antibiotic concentrations were chosen that led to a reduction in growth rate by ~50% compared to the untreated control.

Preparation of cytoplasmic (^{35}S)-L-methionine-labeled protein fractions

Radioactive labeling was performed as described previously (9). In short, 5 ml of a bacterial culture in early exponential growth phase were exposed to 22.5 µg/ml MP196, 50 µg/ml D-MP196, or 1 µg/ml MP276 respectively, or left untreated as control. After 10 min of antibiotic stress cells were pulse-labeled with (^{35}S)-L-methionine for additional 5 min. Radioactive incorporation was stopped by inhibition of protein biosynthesis by chloramphenicol and an excess of cold methionine. Cells were harvested by centrifugation, washed three times in Tris buffer and disrupted by ultrasonication.

2D-PAGE

2D gels were prepared as described previously (9). In short, 55 µg of protein for analytical and 300 µg for preparative gels were loaded onto 24 cm immobilized pH gradient (IPG) strips pH 4-7 (GE Healthcare) by passive rehydration for 18 h. Proteins were separated in a first dimension by isoelectric focusing and in a second dimension by SDS-PAGE using 12.5% acrylamide gels. Analytical gel images were analyzed as described by Bandow *et al.* (10) using Decodon Delta 2D 4.1 image analysis software (Decodon, Greifswald, Germany). Proteins found to be induced more than two-fold in three independent biological replicates were defined as marker proteins. Protein spots were manually excised from preparative 2D gels and transferred into 96 well microtiter plates. Tryptic digest with subsequent spotting on a MALDI target was carried out automatically with the Ettan Spot Handling Workstation (Amersham Biosciences, Uppsala, Sweden) as described by Eymann *et al*. (11). MALDI-ToF as well as MALDI-

ToF-ToF measurements were carried out on a 4800 MALDI-ToF/ToF Analyzer (Applied Biosystems, Foster City, CA, USA) as described previously (9). For the five most intense peaks in the MS spectra, MS/MS data was obtained. Peak lists were generated using the "peak to mascot" script of the 4000 Explorer Software V3.5.3 and searched against an in house strain-specific *B. subtilis* 168 sequence database with 4767 entries downloaded from UniProt (May 2nd, 2008) using the Mascot search engine Version 2.1.04 (Matrix Science Ltd, London, UK). Search parameters allowed for one missed cleavage. Carbamidomethylation of cysteine was defined as fixed modification, oxidation of methionine as variable modification. Mass tolerance of precursor ions was set to 50 ppm, and known contaminants were excluded. Protein scores, -10*Log(P), where P is the probability that the observed match is a random event, are derived from ion scores as a non-probabilistic basis for ranking protein hits. Protein scores higher than 49 were considered significant (significance threshold $p<0.05$).

Protein spots, which could not be identified by MALDI-ToF/ToF (indicated by asterisks in the **SI Appendix, Tab. S2**) were identified using a Synapt G2S high definition mass spectrometer equipped with a lock spray source for electrospray ionization and a ToF detector (Waters, Milford, MA, USA). Manually excised protein spots were destained with 20 mM ammoniumbicarbonate/30% acetonitrile, dried completely, and subsequently tryptically digested (6.25 ng/µl, Promega, Fitchburg, WI, USA). Peptides were eluted into ultrapure water by 15 min of ultrasonication. Eluates were loaded on a trap column (C_{18}, pore size 100 Å, particle diameter 5 µm, inner diameter 180 µm, length 20 mm) and were then eluted using gradients of acetonitrile with 0.1% formic acid (350 µl/min, linear gradient 2-60% in 40 min) from an analytical column at 50 °C (C_{18}, pore size 130 Å, particle diameter 1.7 µm, inner diameter 75 µm, length 150 mm) to be subjected to mass spectrometry. Spectra were recorded in positive resolution mode over a mass range of 50 to 1800 m/z with 1 s/scan. The following parameters were used for the NanoLockSpray source: capillary voltage, 3.3 kV; sampling cone voltage, 30 V; source temperature, 80 °C; desolvation temperature, 200 °C; cone gas flow; 50 L/h; desolvation gas flow, 600 L/h. (Glu1)-Fibrinopeptide B serving as lock mass analyte was fed through the lock spray channel (lock mass capillary voltage, 3.2 V). Analysis of the spectra was performed using MassLynx V4.1 SCN813.

Preparation of $^{15}N/^{14}N$-labeled membrane proteome fractions

For gel-free proteome analysis of membrane proteins *B. subtilis* 168 was grown aerobically at 37 °C in BMM supplemented with either ^{15}N-ammonium sulfate/^{15}N-L-tryptophan (0.078 mM, 98 atom % excess, Cambridge Isotope Laboratories, Andover, USA) or ^{14}N-ammonium sulfate and ^{14}N-L-tryptophan. Cells were harvested by centrifugation either with antibiotic stress imposed at an optical density at 500 nm of 0.4 for 65 min or as a control directly before setting of the stress. Mixing of cell extracts prior to subcellular fractionation steps for relative quantification was carried out according to Otto *et al.* (12). The enriched membrane protein fraction was prepared according to the workflow published in Eymann *et al.* (11) omitting the n-dodecyl-β-D-maltoside treatment step. Preparation of integral membrane peptides (membrane shaving fraction) was carried out as described by Wolff *et al.* (13).

ESI-MS measurement

Sample preparation, mass spectrometric measurement for both the enriched membrane protein and membrane shaving fractions, and subsequent data analysis (protein identification and relative quantitation) were carried out as described by Otto *et al.* (12). Logarithmic peak intensities (ratio to the ^{15}N-labelled standard culture) were normalized to the median of the respective datasets. The cutoff for significant protein upregulation was set to a lognorm change of 0.35, representing the maximal biological variation between different control cultures in >99% of the data points.

Transmission electron microscopy

Cells were grown in BMM to an OD_{500} of 0.35. The main culture was then subdivided into 50 ml aliquots and subcultures were treated with the respective antibiotics for 15 min or left untreated as control. Cells were harvested by centrifugation and washed twice in 100 mM Tris/1 mM EDTA, pH 7.5 and subsequently washed once in the same buffer without EDTA. Preparation of bacterial samples for TEM was performed according to Santhana Raj *et al.* (14) with some modifications. Cells were fixed in 2% glutaraldehyde for 20 min, washed twice with double-distilled water, and subsequently incubated with 2% uranyl acetate for 5 min Samples were then washed twice with double-distilled water and stained with 2% osmium tetroxide. Cells were centrifuged down and excess of osmium tetroxide solution was discarded. Samples were then dehydrated by an incubation series with 50%, 70%, 90%, and 100% acetone for 5 min

each. Cells were subsequently incubated with 1:1 acetone/epoxy resin for 15 min and then embedded in pure epoxy resin. For preparation of the epoxy resin, solution A (38% Epon 812/62% dodecyl succinic anhydride) was mixed with solution B (47% epon 812/53% methylnadic anhydride) at a ratio of 3:7. To this mixture tris-2,3,6-(dimethylaminomethyl)phenol (DMP30) was added to a final concentration of 1.5% to accelerate polymerization. Polymerization was performed at 75 °C for 18 h. Blocks were trimmed, cut to 50 nm ultrathin sections and mounted on Formvar-coated (R1201, Plano, Wetzlar, Germany), 75 mesh thin bar copper grids (Stork Veco, Eerbeek, Nertherlands). Samples were either stained with 0.2 % lead citrate in 0.1 M NaOH for 3 seconds or, in the case of peptide-tracing with MP276, remained unstained. Samples were examined at 23,000 - 230,000 magnification with a Philips EM410 transmission electron microscope (Philips, Eindhoven, Netherlands) equipped with a Gatan (Pleasanton, CA, USA) digital camera system at an accelerating voltage of 80 kV.

Graphite furnace atomic absorption spectrometry

Cells were grown in BMM until early exponential growth phase. Cultures were divided and 50 ml aliquots were either stressed with the ruthenocene-substituted MP276 or left untreated as controls. After 15 min of antibiotic stress, cells were harvested at 3,320 x g, washed five times with 100 mM Tris/1 mM EDTA, pH 7.5, resuspended in 10 mM Tris, pH 7.5 and disrupted by ultrasonication in a Vial Tweeter instrument (Hielscher, Teltow, Germany). The washing solution was collected at each washing step and subjected to ruthenium measurement. Cell debris was separated from the cytosolic/membrane-containing fraction by centrifugation at 16,100 x g. The resulting pellet containing the cell wall was dissolved in 10 mM Tris, pH 7.5. The membrane fraction was separated from the cytosolic fraction by ultracentrifugation at 150,000 x g for 4 h. The cytosolic fraction was collected and the membrane pellet was dissolved in 10 mM Tris, pH 7.5. All fractions were lyophilized at -20 °C for 24 h in a Freeze Dryer BETA I instrument (Martin Christ, Osterode, Germany). Ruthenium contents were quantified using graphite furnace atomic absorption spectroscopy following a previously described procedure (15-17). Briefly, samples were dissolved in 2 ml of double-distilled water. For ruthenium determination, samples of 160 µl were stabilized by addition of 20 µl of Triton X-100 (final concentration 1%) and 40 µl of 1 N HCl and measured immediately. Standards for

calibration purposes were prepared as aqueous dilutions from a MP276 stock (1 mg/ml in DMSO). A Vario 6 graphite furnace atomic absorption spectrometer (Analytik Jena, Jena, Germany) was used for ruthenium quantitation. Ruthenium was detected at a wavelength of 349.9 nm with a bandpass of 0.5 nm. A deuterium lamp was used for background correction. A volume of 25 µl was injected into the graphite tubes. Drying, pyrolysis, and atomization in the graphite furnace were performed according to published procedures (16,17). The mean areas under the curve (AUC) of peaks in the absorption spectra of duplicate injections were used throughout the study. Compartment concentrations were calculated based on cyro-electron microscopy results by Matias and Beveridge (cytosolic volume 3.09 x 10^{-9} µl, membrane volume 8.99 x 10^{-11} µl, cell wall volume 8.08 x 10^{-10} µl) (18,19).

Differential scanning calorimetry (DSC)

1,2-Dipalmitoyl-*sn*-glycero-3-phosphoglycerol (Na-salt) (DPPG), 1,2-Dipalmitoyl-*sn*-glycero-3-phosphoethanolamine (DPPE), and 1,2-Dipalmitoyl-*sn*-glycero-3-phosphocholine were purchased from Avanti Polar Lipids Inc. (Alabaster, AL, USA). Peptides were dissolved in phosphate buffered saline (PBS, 20 mM NaPi, 130 mM NaCl, pH 7.4) at a concentration of 3 mg/ml before each experiment. Aqueous dispersions of lipids of 0.1% (w/w) in PBS buffer were prepared before measurement in the presence (lipid-to-peptide molar ratio of 25:1 and 120:1) and absence of peptides. The respective liposomes were always prepared 10-15 °C above the phase transition temperature by vigorous mixing at certain time points. For the preparation of DPPG liposomes we followed a protocol described by Zweytick *et al*. (20). Lipid films of DPPE and DPPG/DPPE 88:12 (w/w) were hydrated at 70 °C for 2 h. For the mixture a freeze thaw protocol was used to increase homogenous mixing. DSC experiments were performed with a differential scanning calorimeter (VP-DSC) from MicroCal, Inc. (Northampton, MA, USA). Heating scans were performed at a scan rate of 30 °C/h with a final temperature approximately 10 °C above the main transition temperature (T_m) and cooling scans at the same scan rate with a final temperature about 20 °C below T_m. The heating/cooling cycle was repeated twice, pre-scan thermostating was allowed for 15 min for the heating scans and 1 min for the cooling scans. Enthalpies were calculated by

integrating the peak areas after normalization to phospholipid concentration and baseline adjustment using the MicroCal Origin software (VP-DSC version).

Fluorescence microscopy assay for pore formation

Pore formation was monitored using the Live/Dead BacLight bacterial viability kit (Invitrogen, Carlsbad, CA, USA) following the manufacturer's instructions. *B. subtilis* 168 was grown at 37 °C in BMM under steady agitation until early exponential phase. The main culture was split and aliquots were treated with 22.5 µg/ml MP196, 0.75 µg/ml nisin, 1 µg/ml gramicidin S 10 µg/mL valinomycin, or left untreated as control. After 15 min of antibiotic stress, 2 µl of a 1:1 mixture of the green and red-fluorescing dyes were added per ml of culture and incubated for 15 min in the dark under steady agitation. Cells were washed with 100 mM Tris/1 mM EDTA, pH 7.5 and resuspended in the same buffer. 5 µl of the cell suspension were imaged without fixation or immobilization in fluorescent mode as described before (21). Single channel pictures were combined using the Cell software (Olympus, Hamburg, Germany). Background correction was performed applying the same constant (25) for all images.

Potassium release assay

Potassium efflux experiments were performed as described previously (21) with minor modifications. Briefly, *B. megaterium* ATCC 13632 was grown in half MH to an OD_{500} of 1.0 to 1.5, washed with 50 ml cold choline buffer, and resuspended in the same buffer to an OD_{500} of 30. For each measurement, cells were diluted in choline buffer (25 °C) to an OD_{500} of about 3. Nisin was applied at 3.35 µg/ml (1 µM). MP196 at 125 µg/ml (80 µM), which is equivalent to 50x MIC. No effect was seen with lower MP196 concentrations (2x, 10x MIC). A control culture was left untreated. Potassium efflux was monitored using a pH-meter pH 213 (Hanna Instruments, Kehl am Rhein, Germany) with an MI-442 potassium electrode and an MI-409F reference electrode. Before each experiment, the electrodes were calibrated with standard solutions containing 0.01, 0.1, or 1 mM KCl. Calculations of potassium efflux in percent were performed according to Orlov *et al*. (22). Antibiotic-induced leakage was monitored for 5 min with values taken every 10 seconds and expressed relatively to the total amount of potassium release induced by nisin.

Ionomics by inductively coupled plasma atomic emission spectroscopy

For ionomics only metal-free plastic ware and ultrapure water (Bernd Kraft, Duisburg, Germany) were used. All centrifugation steps were performed for 2 min to reduce sample handling time. *B. subtilis* 168 was grown in BMM until early exponential growth phase. For determination of ion concentrations of cells stressed in medium, subcultures were directly treated with 22.5 µg/ml MP196, 1 µg/ml gramicidin S, and 10 µg/ml valinomycin, respectively, or left untreated as a negative control. After 15 min of antibiotic treatment (proteomic conditions), cells were harvested by centrifugation, washed twice in 100 mM Tris/1 mM EDTA, pH 7.5 and washed once in 100 mM Tris, pH 7.5.

Cell pellets were completely dissolved in 2.5 ml 65% nitric acid (Bernd Kraft, Duisburg, Germany) and incubated at 80 °C for 16 h. Dissolved samples were filled up with ultrapure water (Bernd Kraft, Duisburg, Germany) to 10 ml. Elemental concentrations were determined by inductively coupled plasma atomic emission spectroscopy using an iCAP 6300 Duo View ICP Spectrometer (Thermo Fisher Scientific, Waltham, MA, USA). Liquid calibration standards from 10 µg/l to 10 mg/l of each element of interest (Bernd Kraft, Duisburg, Germany) were run before each series of measurement and selected standards were additionally run every 20 samples as a quality control. Resulting element concentrations were converted into intracellular ion concentrations based on calculation of the cytosolic volume of *B. subtilis*. This volume was taken to be 3.09×10^{-9} µl based on average rod size and *B. subtilis* cell wall and membrane thickness were determined by cryo-electron microscopy by Matias and Beveridge (18,19).

Depolarization assay based on GFP-MinD localization

Localization assays were performed with *B. subtilis* 1981 GFP-MinD (23) as described previously (21). In short, cells were grown over night in BMM and then inoculated in modified BMM containing xylose instead of glucose to induce GFP-MinD expression. Cultures were grown until early exponential growth phase, and subsequently stressed with 22.5 µg/ml MP196, 1 µg/ml gramicidin S or left untreated. After 15 min of antibiotic exposure, cells were imaged in fluorescent mode without fixation or immobilization.

$DiSC_35$-based membrane potential measurement

Determination of membrane potential changes was performed as described by Andrés and Fierro (24) using the membrane potential-sensitive fluorescent dye 3,3′-dipropylthiadicarbocyanine iodide ($DiSC_35$, Sigma-Aldrich, St. Louis, MO, USA). In short, *Bacillus megaterium* ATCC 13632 was grown in half-concentrated MH to an OD_{600} of 0.5 and subsequently incubated for 5 min with 3 µM $DiSC_35$. Samples were then treated with 3.3 µg/ml nisin or 25 µg/ml MP196, respectively, or left untreated as control. Fluorescence was measured continuously for 5 min at 651 nm excitation and 675 nm emission wavelengths using a Shimadzu RF-5301PC Spectrofluorometer (Shimaduzu, Duisburg, Germany).

Determination of cellular ATP levels using luciferase assay

B. subtilis 168 was grown in BMM until reaching an OD_{500} of 0.35 and subsequently exposed to 22.5 µg/ml MP196, 0.75 µg/ml nisin, 10 µg/ml valinomycin, 1 µg/ml gramicidin S, and 0.5 µg/ml erythromycin (negative control) for 15 min or left untreated. After stress, cells were harvested by centrifugation, resuspended in 500 µl 10 mM Tris, pH 7.5, and disrupted by ultrasonication. ATP determination was performed using the Perkin Elmer ATPlite 1step assay kit (Waltham, MA, USA) following the manufacturer's instructions. ATP standards were prepared from 1×10^{-7} to 8.5×10^{-7} mol ATP in the provided buffer. For determination of cellular ATP levels 100 µl of cytosolic cell extracts were used. All measurements were performed in quintuple biological and double technical replicates using the Tecan Infinite 200 PRO multimode reader (Tecan, Männedorf, Switzerland).

H^+-ATPase and respiratory chain inhibition assays using inverted vesicles from *M. flavus*

Preparation of inverted vesicles

Inverted vesicles were prepared from *M. flavus* according to Burstein *et al*. (25) with some modifications. Briefly, cells were grown in tryptic soy broth until exponential growth phase. One liter of culture was harvested and washed with 100 ml Tris buffer (50 mM Tris-HCl, 2 mM $MgCl_2$, 0.5 mM dithiothreitol, 0.5 mM EDTA, pH 8.0). The cell pellet was resuspended in 5 ml Tris buffer, followed by pH readjustment to 8.0 and addition of each

10 µg/ml DNase and RNase. Cells were disrupted mechanically in a Precellys 24 homogenizer using 0.1 mm glass beads (Bertin Technologies, Montigny-le-Bretonneux, France). The crude homogenate was centrifuged at 30,000 x g for 20 min. The resulting supernatant was subsequently centrifuged at 175,000 x g for 120 min. The resulting vesicle-containing pellet was resuspended in 2 ml Tris buffer supplemented with 10% glycerol and stored in liquid nitrogen until usage.

Determination of proton uptake

Proton uptake into inverted *M. flavus* vesicles was measured in a microtiter plate assay in a final volume of 200 µl based on the pH-sensitive probe acridine orange as described by Palmgren *et al*. (26). The reaction mixture (20 µM acridine orange, 4 mM $MgCl_2$, 10 mM MOPS-BTP (pH 7.0), 140 mM KCl, 1 mM EDTA, 1 mM DTT, 1 mg/ml BSA (essentially fatty acid free), 2.5 µg/ml valinomycin, 75 µg/ml vesicle protein) was preincubated with 20 µM MP196, 20 µM nisin, 20 µM lactoferrin or left untreated as control, respectively, at 25 °C for 30 min. The reaction was initiated by addition of 2mM ATP-BTP and absorbance was measured at 495 nm for 6 h using a SunriseTM multichannel plate reader (Tecan, Männedorf, Switzerland).

Determination of respiratory chain activity based on INT reduction

Antibiotic influence on the bacterial electron transport chain was monitored by reduction of iodonitrotetrazolium chloride (INT) using *M. flavus* inverted vesicles as described by Smith and McFeters (27). 20 µg of vesicle protein were preincubated for 30 min in pure phosphate buffer (10 mM potassium phosphate, 5 mM magnesium acetate, pH 6.5) or buffer with 40 µM of MP196, 40 µM nisin, 100 µM antimycin A, or 5 mM rotenone, respectively. Subsequently, 1 mM INT and 0.6 mM NADH or 10 mM succinate were added as substrate and the solution was incubated for 1 h at 25 °C in the dark. INT reduction was stopped by addition of 5% TCA. Insoluble formazan was pelleted for 5 min at 13,000 x g, extracted with 1 ml ethanol and centrifuged again to remove insoluble particles. Absorbance of the supernatant was measured at 485 nm.

SDS-PAGE and Western blot for detection of cytochrome *c* and MurG

B. subtilis 168 was grown in BMM until early logarithmic growth phase. To investigate the effect of the antimicrobial peptides *in vivo*, cells were subsequently treated with 22.5 µg/ml MP196, 1 µg/ml gramicidin S, or left untreated as control. Cells were harvested by

centrifugation, washed three times in washing buffer (100 mM Tris/1 mM EDTA, pH 7.5), and resuspended in disruption buffer (10 mM Tris, pH 7.5). Cells were disrupted by ultrasonication, cell debris was removed by centrifugation, and cell extracts were subjected to ultracentrifugation at 150,000 x g for 4 h. The resulting membrane pellet was dissolved in washing buffer. Protein concentrations were determined by a Bradford-based assay (Roti-Nanoquant, Carl Roth, Karlsruhe, Germany) according to the manufacturer's instructions. 30 µg of protein were loaded onto a 15% SDS polyacrylamide gel and proteins were separated at 120 V.

To determine effects of peptide treatment on membranes *in vitro*, the membrane fractions of untreated cells were prepared as described above. Prior to SDS-PAGE membrane fractions from 50 ml of a logarithmic *B. subtilis* culture were incubated with 22.5 µg/ml MP196, 1 µg/ml gramicidin S, or left untreated.

After 5 min of antibiotic treatment, aliquots containing 30 µg of membrane protein was loaded on SDS gels. For detection, proteins were then blotted onto a nitrocellulose membrane (Hybond, GE Healthcare, Uppsala, Sweden) at 250 mA and 25 V per blot for 2 h. Membranes were stained with Ponceau S prior to antibody detection to control equal sample loading. Subsequently, membranes were destained in TBST (100 mM Tris, 150 mM NaCl, 0.1% Tween 20, pH 7.5), blocked with 3% non-fat dried milk powder in TBST for 2 h, and subsequently incubated with a rabbit anti-(*E. coli*-)MurG-His antibody (28) in a 1:10,000 dilution in TBST with 1% milk powder for 18 h. Membranes were then washed three times in TBST with 3% milk powder, incubated with a goat anti-rabbit IgG-HRP secondary antibody (Bio-Rad, Berkeley, CA, USA) in a 1:3,000 dilution in TBST with 3% milk powder for 1 h, washed three times with TBST and were then covered with chemiluminescence reagent (Luminata Forte Western HRP Substrate, Merck Millipore, Darmstadt, Germanay). Signals were detected with a FluorChem Imaging Workstation (Alpha Innotech, now part of Proteinsimple, Santa Clara, CA, USA). Quantification of band intensity was performed with the ImageQuant TL 1D analysis software (GE Healthcare, Uppsala, Sweden). The same membranes were analogously used for cytochrome *c* detection using a mouse anti-(pigeon-)cytochrome *c* antibody (7H8.2C12, abcam, Cambridge, UK) at a final concentration of 2.5 µg/ml and a goat anti-mouse IgG-HRP secondary antibody (Bio-Rad, Berkeley, CA, USA).

Light microscopy-based cell wall integrity assay

Sample preparation and microscopic inspection of the cell shape was performed as described previously (21). Briefly, *B. subtilis* 168 was grown in BMM until early exponential growth phase and subsequently treated with 22.5 µg/ml MP196, 0.75 µg/ml nisin, or left untreated as control. After 15 min of antibiotic stress cells were fixed in a 1:3 mixture of acetic acid and methanol, immobilized in low melting agarose, and subjected to bright field microscopy.

***In vitro* lipid II synthesis assay**

In vitro lipid II synthesis was performed using *Micrococcus flavus* DSM 1790 membrane preparations as described by Schneider *et al*. (5), adding (^{14}C)-UDP-N-acetyl-D-glucosamine (GlcNAc) to label newly synthesized lipid II. Membranes were isolated from lysozyme-treated cells by centrifugation at 40,000 x g, washed twice in washing buffer (50 mM Tris-HCl, 10 mM $MgCl_2$, pH 7.5) and frozen in liquid nitrogen. *In vitro* lipid II synthesis was performed in a total volume of 75 µl using 400 µg of membrane protein, 5 nmol C55-P, 50 nmol UDP-N-acetylmuramylpentapeptide (UDP-MurNAc-PP, purified according to Kohlrausch and Höltje (29)), and 50 nmol (^{14}C)-UDP-GlcNAc in reaction buffer (60 mM Tris-HCl, 5 mM $MgCl_2$, 0.5% (w/v) triton X-100, pH 8.0). Peptides were added in a 2:1 molar ratio to C55-P and incubated with the reaction mixture for 1 h at 37 °C. Subsequently, lipid extraction was performed by addition of 75 µl 2:1 n-butanol/6 M pyridine-acetate, pH 4.2. Lipids were separated by thin layer chromatography using 60F254 silica plates (Merck, Darmstadt, Germany) and chloroform/methanol/water/ammonia (88:48:10:1) as solvent as described by Rick *et al*. (30). Radiolabeled spots were visualized using a Storm 820 Phosphor Imager (Amersham Biosciences, Uppsala, Sweden). Image analysis was performed using the ImageQuant TL v2005 software (Nonlinear Dynamics Ltd, Newcastle Upon Tyne, UK).

Lipid II-binding assay

For *in vitro* lipid II binding of peptides were incubated with 2 nmol lipid II in molar ratios 1:1. Reaction mixtures were incubated at 30 °C for 30 min and applied onto TLC plates (TLC Silica Gel 60 F_{254}, Merck, Darmstadt, Germany). Chromatography was performed

in chloroform-methanol-water-ammonia (88:48:10:1) (30) and stained with phosphomolybdic acid stain and 140 °C (PMA).

Determination of UDP-MurNAC-pentapeptide accumulation

Accumulation of UPP-MurNac was analysed by HPLC as described by Schmitt *et al.* (31). *S. simulans* 22 was grown in MH broth to an OD_{600} of 0.5. 130 µg/ml chloramphenicol were added in order to prevent induction of autolysis and *de novo* synthesis of enzymes hydrolyzing the nucleotide-activated sugars interfering with determination of the soluble precursor (32). After 15 min, 5 µg/ml MP196 and 0.7 µg/ml vancomycin were added. After 30 min of incubation with the respective peptides cells were harvested and boiled in water. Insoluble components were removed by centrifugation at 13,000 × g for 5 min. Supernatants were adjusted to pH 2 with H_3PO_4, filtered through cellulose acetate filters (pore size 0.2 µm) and analyzed by RP-HPLC in 50 mM sodium phosphate buffer, pH 5.2, developed in isocratic mode over 30 min at a flow rate 1 ml/min on a Nucleosil 100-C18 column (Schambeck SFD GmbH, Bad Honnef, Germany).

Amino acid analysis (AAA)

B. subtilis 168, JH642, and SMB80 (33) were grown in BMM until an OD_{500} of 0.35, harvested by centrifugation (3,220 x g, 10 min, 37 °C), and washed three times in pre-warmed AAA buffer (10.2 mM Na_2HPO_4, 1.8 mM KH_2PO_4, 25.8 mM KCl, 4.3 mM NaCl). Cells were then resuspended in AAA buffer, readjusted to an OD_{500} of 0.35, and stressed with 22.5 µg/ml MP196, 1 µg/ml gramicidin S, 0.75 µg/ml nisin, or 10 µg/ml valinomycin for 15 min or left untreated as control, respectively. Hypoosmotic stress was set by resuspending the cells in double distilled water, hyperosmotic stress by resuspending in AAA buffer containing 6% NaCl, followed by 15 min incubation at 37 °C. Subsequently, cells were harvested by centrifugation (16,100 x g, 10 min, 4 °C). The supernatant was kept for measurement of amino acid leakage whereas the cells were washed three times in AAA buffer (16,100 x g, 10 min, 4 °C), resuspended in the same buffer and disrupted by ultrasonication as described above. In order to analyze only free amino acids, proteins were precipitated with acetone in both intra- and extracellular fractions. Therefore, 100 µl of cell extract and 200 µl of culture supernatant, respectively,

were mixed with the five-fold volume of ice-cold 80% acetone and incubated over night at -20 °C. Precipitated proteins were pelleted (16,100 x g, 20 min, 4 °C) and the resulting, protein-free supernatant was used for HPLC. 500 µl of the protein-free cell extract and 1 ml of protein-free culture supernatant samples, respectively, were dried completely in AAA glass tubes and subsequently dissolved in 10 µl of 20 mM HCl. Amino acid analysis was performed using the Acquity HPLC and AccQ-Tag Ultra system (Waters GmbH, Milford, MA, USA) according to the manufacturer's instructions. In short, 10 µl AccQ-Tag reagent and 30 µl internal norvalin standard (final concentration 10 pmol/µl) was added to the samples for derivatization. Those samples were then incubated for 10 min to allow conversion of primary and secondary amines into stabile derivatives. Amino acid derivatives were separated using an AccQ-Tag Ultra RP column and detected by an Acquity UPLC-TUV detector (Waters GmbH, Eschborn, Germany). Amino acids were quantified using 10 pmol/µl amino acid standards. Intracellular amino acid concentrations were calculated based on the *B. subtilis* cellular volume as described above.

Minimal inhibitory concentration (MIC) dependence on glutamate and salt concentration

MIC determination of MP196 under different glutamate and salt concentrations was performed in a microtiter plate assay in modified BMM containing rising concentrations of glutamate (0, 4.5, 45, 450, 3000 mM), NaCl (0, 10, 100, 500, 1000 mM), or KCl (0, 100, 500 mM, cells did not survive 1000 mM KCl). BMM without glutamate was additionally supplemented with 4.5 mM ammonium nitrate as alternative nitrogen source. 200 µl of medium were inoculated with $5x10^5$ cells/ml of *B. subtilis* 168, *B. subtilis* JH642 (*trpC2 pheA1*), or SMB80 (*trpC2 pheA1 mscL yhdY ykuT yfkC*) (33) and incubated with different antibiotic concentrations for 18 hours at 37 °C. The MIC was defined as the lowest antibiotic concentration inhibiting visible growth.

ii) Results of the comparative proteome analysis

Proteomic analyses were performed using *B. subtilis* 168, for which a library of proteome response profiles to over 50 antibiotic agents exists (9,21,34,35). Cultures were stressed with sublethal peptide concentrations (**SI Appendix, Fig. S2**) prior to analysis of the cytosolic and membrane proteome. After 10 min of exposure to the peptide, newly synthesized proteins were pulse labeled with L-(^{35}S)-methionine for five min and analyzed by 2D gelelectrophoresis. Thirty-six proteins were selectively upregulated in response to MP196 treatment, 32 of which were identified by mass spectrometry (**Fig. 1c**, **SI Appendix, Tab. S1** and **S2**). In parallel, the membrane proteome response was analyzed by LC-ESI-MS/MS. Differential ^{14}N/^{15}N labeling was used for relative quantitation of proteins in the membrane fractions of untreated and peptide-treated cultures. After 65 min of peptide treatment, 178 proteins were upregulated at least two-fold (**SI Appendix, Tab. S3** and **S4**). Most differentially regulated proteins are associated with membrane functions, including the general cell envelope stress response, membrane stress response, cell wall biosynthesis, lipid biosynthesis, and energy metabolism.

The tellurium resistance protein, YceC, and toxic anion resistance protein, YceH, previously described as marker proteins for both membrane and cell wall stress (21), were upregulated, along with six other proteins regulated by the cell envelope-responsive alternative sigma factors W (σ^W) and M (σ^M). PspA, a homologue of LiaH, which protects cell envelope integrity by binding to the cytoplasmic membrane (36,37), is specifically upregulated following membrane stress, as opposed to peptidoglycan stress (21). Other proteins upregulated in response to MP196 are involved in restructuring of the membrane lipid composition. Among these are proteins involved in fatty acid biosynthesis (FabG and AcpA), alternative fatty acid biosynthesis (YjdA and YoxD), phospholipid biosynthesis (PlsX), lipid-degradation (FadE), and membrane fluidity control (FloT). NAD synthase (NadE) is crucial for energy metabolism and, together with PspA, constitutes a proteomic signature for membrane-mediated stress (21). Other proteins, whose upregulation indicates substantial energy limitation, are involved in glycolysis, the TCA cycle, oxidative phosphorylation, NAD metabolism, and ATP synthesis. Similarly, ATP-requiring proteins including several ABC transporter and

ATP-binding protease subunits were upregulated. And while biosynthesis of housekeeping proteins was largely down-regulated after MP196 treatment, elongation factors Tu and G, which require GTP for activity, were upregulated.

Other notable proteins upregulated included LiaH, the ABC transporter protein YtrE, and the tRNA-modifying enzyme TrmB, which are specific markers for interference with the membrane-bound steps of cell wall biosynthesis (21). Upregulation of MurAA, MurAB, and MurG, enzymes leading up to the synthesis of cell wall precursor lipid II, indicates inhibition of cell wall biosynthesis, as does upregulation of MreB, which is important for localization of the cell wall biosynthesis and cell division machineries, and of the MreB-like protein Mbl. The amino acid racemase RacX and proteins belonging to the *dlt* operon were upregulated. They are involved in cell envelope modification by synthesis of D-amino acids, probably feeding into D-alanylation reactions and lipoteichoic acid biosynthesis, respectively. Also, many proteins involved in amino acid biosynthesis were upregulated, particularly those involved in glutamate and aspartate anabolism.

The proteome analysis prompted the following questions about MP196: Does it interact with the bacterial membrane and, if so, how? How does it influence energy metabolism? How does it affect cell wall biosynthesis? What is the significance of the strong upregulation of amino acid biosynthesis proteins?

The proteome analysis further provided evidence for mechanisms by which *B. subtilis* counteracts peptide-mediated membrane stress (**SI Appendix, Fig. S9c**). One survival strategy is to adapt membrane lipid composition (**SI Appendix, Fig. S9c.I**). Following exposure to MP196, the branched-chain amino acid valine, which is needed as precursor molecule for branched-chain fatty acids, accumulates in the cytosol. Changing the membrane lipid composition by modulating branched-chain fatty acids may interfere with the peptide-membrane interaction. Previous experiments have suggested this: in response to a ferrocene-conjugated MP196 derivative, *Corynebacterium glutamicum* altered the phospholipid headgroups by reducing negatively charged phosphatidylglycerol lipids and increasing uncharged diaglycerol lipids. This impeded attachment of the peptide to the membrane. In addition, cardiolipin levels were

increased, giving the membrane a more rigid structure, which further obstructed peptide integration (38).

We also observed the induction of FloT, a protein controlling membrane fluidity that is involved in orchestrating physiological processes in lipid microdomains (39). Upregulation of this protein underscores the importance of membrane properties and indicates that *B. subtilis* alters membrane architecture to counteract impairment of membrane-associated physiological processes.

As western analysis showed, the peripheral membrane protein MurG is released from the membrane upon MP196 treatment. After 65 min MurG levels are found to be strongly upregulated in the membrane fraction, suggesting that at this time MurG again localizes at the membrane and *B. subtilis* (over-)compensates the loss in protein level caused by delocalization.

Additional bacterial adaptation strategies were observed (**SI Appendix, Fig. S9c.II-IV**). First, induction of the *dlt* operon and the RacX protein suggest that there is adjustment of the bacterial cell wall by enhancing wall teichoic acid D-alanylation, to restrict access of the peptide to the membrane. This is a common survival strategy, observed in daptomycin and vancomycin-resistant *Staphylococcus aureus* strains and antimicrobial peptide-resistant Group B *Streptococci* (40-43). Second, the LiaRS cell wall biosynthesis stress response and the σ^W-mediated membrane stress response were strongly upregulated. The LiaH protein forms ring-like multimeric structures and binds to the inner surface of the cytoplasmic membrane upon lipid II-mediated cell wall biosynthesis inhibition (36). It is thought that this stabilizes the membrane. The σ^W-controlled PspA protein is a homologue of LiaH, which fulfils the same stabilizing function when the membrane is damaged (28). Upregulation of both PspA and LiaH reflects the duality of the MP196 mode of action: it impairs membrane function and cell wall biosynthesis.

iii) Results of cell wall biosynthesis inhibition assays

Glucosamine incorporation was partially inhibited by MP196 (**Fig. 1a**). Glucosamine serves as precursor for N-acetyl-glucosamine (GlcNAc), which feeds into cell wall biosynthesis both at an early cytosolic step leading to UDP-N-acetylmuramic acid (UDP-MurNAc) and at a later membrane-associated step where lipid II is formed. The membrane extrusions are suggestive of inhibition of cell wall biosynthesis at the level of lipid II (5). However, MP196 did not impair lipid II synthesis in an *in vitro* assay using concentrated cell lysate (**SI Appendix, Fig. S7c**). Furthermore, while nisin bound lipid II *in vitro*, preventing it from migrating in the thin layer chromatography matrix, MP196 did not affect lipid II migration (**SI Appendix, Fig. S7b**). HPLC analysis showed that MP196 exposure led to an accumulation of UDP-MurNAc pentapeptide in the intact cell (**SI Appendix, Fig. S7a**), albeit not to the same extent as vancomycin, showing that the cytosolic cell wall biosynthesis steps are largely unaffected. These assays suggest that lipid II is not synthesized efficiently in intact cells.

iv) References

1. Chantson JT, Varga Falzacappa MV, Crovella S, Metzler-Nolte N (2006) Solid-phase synthesis, characterization, and antibacterial activities of metallocene-peptide bioconjugates. *ChemMedChem* 1(11):1268-1274.
2. Bonelli RR, Schneider T, Sahl HG, Wiedemann I (2006) Insights into *in vivo* activities from gallidermin and epidermin mode-of-action studies. *Antimicrob Agents Chemother* 50(4): 1449-1457.
3. Wadhwani P, Afonin S, Ieronimo M, Buerck J, Ulrich AS (2006) Optimized protocol for synthesis of cyclic gramicidin S: Starting amino acid is key to high yield. *J Org Chem* 71(1): 55-61.
4. Pan YL et al. (2007) Characterization of the structure and membrane interaction of the antimicrobial peptides aurein 2.2 and 2.3 from Australian southern bell frogs. *Biophys J* 92(8): 2854-64.
5. Schneider T et al. (2004) *In vitro* assembly of a complete, pentaglycine interpeptide bridge containing cell wall precursor (lipid II-Gly5) of *Staphylococcus aureus*. *Mol Microbiol* 53(2): 675-685.
6. Urban A et al. (2007) Novel whole-cell antibiotic biosensors for compound discovery. *Appl Environ Microbiol* 73(20): 6436-6443.

7. Stülke J, Hanschke R, Hecker, M (1993) Temporal activation of betaglucanase synthesis in *Bacillus subtilis* is mediated by the GTP pool. *J Gen Microbiol* 139(9): 2041-2045.
8. Agnostopoulos C, Spizizen J (1961) Requirements for transformation in *Bacillus subtilis. J Bacteriol* 81(5): 741-746.
9. Wenzel M et al. (2011) Proteomic signature of fatty acid biosynthesis inhibition available *for in vivo* mechanism-of-action studies. *Antimicrob Agents Chemother* 55(6): 2590-2596.
10. Bandow JE et al. (2008) Improved image analysis workflow for 2D gels enables large-scale 2D gel-based proteomics studies - COPD biomarker discovery study. *Proteomics* 8(15): 3030-3041.
11. Eymann C et al. (2004) A comprehensive proteome map of growing *Bacillus subtilis* cells. *Proteomics* 4(10): 2849-2876.
12. Otto A et al. (2010) Systems-wide temporal proteomic profiling in glucose-starved *Bacillus subtilis*. *Nat Commun* 1: 137.
13. Wolff S, Hahne H, Hecker M, Becher, D (2008) Complementary analysis of the vegetative membrane proteome of the human pathogen *Staphylococcus aureus*. *Mol Cell Proteomics* 7(8): 1460-1468.
14. Santhana Raj L et al. (2007) Rapid method for transmission electron microscopy study of *Staphylococcus aureus* ATCC 25923. *Annals of Microscopy* 7, 102-108.
15. Gust R et al. (1998) Stability and cellular studies of (*rac*-1,2-bis(4-fluorophenyl)-ethylenediamine)(cyclo-butane-1,1-dicarboxylato)platinum(II), a novel, highly active carboplatin derivative. *J Cancer Res Clin Oncol* 124(11)*:* 585-597.
16. Schäfer S, Ott I, Gust R , Sheldrick WS **(**2007) Influence of the polypyridyl (pp) ligand size on the DNA binding properties, cytotoxicity and cellular uptake of organoruthenium(II) complexes of the type $((\eta^6\text{-}C_6Me_6)Ru(L)(pp))^{n+}$ (L = Cl, *n* = 1; L = $(NH_2)_2CS$, *n* = 2). *Eur J Inorg Chem* 19: 3034-3046.
17. Schatzschneider U et al. *(*2008) Cellular uptake, cytotoxicity, and metabolic profiling of human cancer cells treated with coordinatively saturated octahedral ruthenium(II) complexes $(Ru(bpy)_2(N\text{-}N))Cl_2$ with N-N = bpy, phen, dpq, dppz, and dppn. *ChemMedChem*. 3(7): 1104-1109.
18. Matias VR, Beveridge TJ **(**2005) Cryo-electron microscopy reveals native polymeric cell wall structure in *Bacillus subtilis* 168 and the existence of a periplasmic space. *Mol. Microbiol*. 56(1): 240-251.
19. Matias VR, Beveridge TJ (2008) Lipoteichoic acid is a major component of the *Bacillus subtilis* periplasm. *J. Bacteriol*. 190(22): 7414-7418.
20. Zweytick D et al. (2006) Influence of N-acylation of a peptide derived from human lactoferricin on membrane selectivity. *Biochim Biophys Acta* 1758(9): 1426-1435.
21. Wenzel M et al. (2012) Proteomic response of *Bacillus subtilis* to lantibiotics reflects differences in interaction with the cytoplasmic membrane. *Antimicrob Agents Chemother* 56(11), 5749-5757.

22. Orlov DS, Nguyen T, Lehrer, RI (2002) Potassium release, a useful tool for studying antimicrobial peptides. *J Microbiol Methods* 49(3): 325-328.
23. Strahl H, Hamoen LW (2010) Membrane potential is important for bacterial cell division. *Proc Natl Acad Sci USA* 107(27): 12281-12286.
24. Andrés MT, Fierro JF (2010) Antimicrobial mechanism of action of transferrins: Selective inhibition of H^+-ATPase. *Antimicrob Agents Chemother* 54(10): 4335-4342.
25. Burstein C, Tiankova L, Kepes A (1979) Respiratory control in *Escherichia coli* K 12. *Eur J Biochem* 94(2): 387-392.
26. Palmgren MG, Sommarin M, Ulvskov P, Larsson C (1990) Effect of detergents on the $H^{(+)}$-ATPase activity of inside-out and right-side-out plant plasma membrane vesicles. *Biochim Biophys Acta* 1021(2): 133-140.
27. Smith JJ, McFeters GA (1997) Mechanisms of INT (2-(4-iodophenyl)-3-(4-nitrophenyl)-5-phenyl tetrazolium chloride), and CTC (5-cyano-2,3-ditolyl tetrazolium chloride) reduction in *Escherichia coli* K-12, *J Microbiol Methods* 29(1): 161-175.
28. Mohammadi T et al. (2007) The essential peptidoglycan glycosyltransferase MurG forms a complex with proteins involved in lateral envelope growth as well as with proteins involved in cell division in *Escherichia coli*. *Mol Microbiol* 65(4): 1106-1121.
29. Kohlrausch U, Höltje JV (1991) One-step purification procedure for UDP-N-acetylmuramyl-peptide murein precursors from *Bacillus cereus*. *FEMS Microbiol Lett* 62(2-3): 253-257.
30. Rick PD et al. (1998) Characterization of the lipid carrier involved in the synthesis of enterobacterial common antigen (ECA) and identification of a novel phosphoglyceride in a mutant of *Salmonella typhimurium* defective in ECA synthesis. *Glycobiology* 8(6): 557-567.
31. Schmitt P et al. (2010) Insight into invertebrate defensin mechanism of action: oyster defensins inhibit peptidoglycan biosynthesis by binding to lipid II. *J Biol Chem* 285(38): 29208-29216.
32. Dai D, Ishiguro EE (1988) MurH, a new genetic locus in *Escherichia coli* involved in cell wall peptidoglycan biosynthesis. *J Bacteriol* 170(5): 2197-2201.
33. Hoffmann T, Boiangu C, Moses S, Bremer S (2008) Responses of *Bacillus subtilis* to hypotonic challenges: physiological contributions of mechanosensitive channels to cellular survival. *Appl Environ Microbiol* 74(8): 2454-2460.
34. Brötz-Oesterhelt H et al. (2005) Dysregulation of bacterial proteolytic machinery by a new class of antibiotics. *Nat Med* 11(10): 1082-1087.
35. Bandow JE, Brötz H, Leichert LI, Labischinski H, Hecker M (2003) Proteomic approach to understanding antibiotic action. *Antimicrob Agents Chemother* 47(3), 948-955.

36. Wolf D et al. (2010) In-depth profiling of LiaR response in *Bacillus subtilis. J Bacteriol* 192(18): 4680-4693.
37. Kobayashi R, Suzuki T, Yoshida M *Escherichia coli* phage-shock protein A (PspA) binds to membrane phospholipids and repairs proton leakage of the damaged membranes. *Mol Microbiol* 66(1): 100-109.
38. Fränzel B et al. (2010) *Corynebacterium glutamicum* exhibits a membrane-related response to a small ferrocene-conjugated antimicrobial peptide. *J Biol Iorg Chem* 15(8): 1293-1303.
39. López D, Kolter R (2012) Functional microdomains in bacterial membranes. *Genes Dev* 24(17): 1893-1902.
40. Weidenmaier C, Peschel A (2008) Teichoic acids and related cell-wall glycopolymers in Gram-positive physiology and host interactions. *Nat Rev Microbiol* 6(4):276-287.
41. Bertsche U, et al. (2011) Correlation of daptomycin resistance in a clinical *Staphylococcus aureus* strain with increased cell wall teichoic acid production and D-alanylation. *Antimicrob Agents Chemother* 55(8):3922-3928.
42. Rose WE, Fallon M, Moran JJ, Vanderloo JP (2012) Vancomycin tolerance in methicillin-resistant *Staphylococcus aureus*: Influence of vancomycin, daptomycin, and telavancin on differential resistance gene expression. *Antimicrob Agents Chemother* 56(8):4422-4427.
43. Saar-Dover R, et al. (2012) D-alanylation of lipoteichoic acids confers resistance to cationic peptides in group B streptococcus by increasing the cell wall density. *PLoS Pathog* 8(9):e1002891.

v) SI Tables

Table S1: Marker proteins induced in the cytosolic proteome

protein ID	protein function	functional category	regulator
SpoVG	negative effector of asymetric septation at the onset of sporulation	sporulation	σ^H
Spo0M	sporulation-control gene	sporulation	σ^W/σ^H
YdaG	general stress protein	general stress	σ^B
YtxH	general stress protein	general stress	σ^B/σ^H
Dps	DNA-protecting protein, ferritin	general stress	σ^B
ClpP	ATP-dependent Clp protease proteolytic subunit	general stress	σ^B
YdbD	manganese-containing catalase	oxidative stress	unknown
AzoR2	azoreductase	oxidative stress	σ^G
YceC	similar to tellurium resistance protein	cell envelope stress	$\sigma^B/\sigma^W/\sigma^M$
YceH	similar to toxic anion resistance protein	cell envelope stress	$\sigma^B/\sigma^W/\sigma^M$
YthP	similar to ABC transporter	cell envelope stress	σ^W
YfhM	similar to epoxide hydrolase	cell envelope stress	σ^B/σ^W
FosB	bacillithiol-S-transferase	cell envelope stress	σ^W
YtrE	similar to ABC transporter	cell envelope stress	YtrA
LiaH	modulator of LiaIHGFSR operon expression	cell wall	LiaRS
DltA	D-alanyl-D-alanine carrier protein ligase	cell wall	$\sigma^D/\sigma^X/\sigma^M$
RacX	amino acid racemase	cell wall	σ^W
PspA	phage shock protein A homolog	membrane	σ^W
YjdA	similar to 3-ketoacyl-acyl-carrier protein reductase	membrane	σ^E
YoxD	similar to 3-oxoacyl-acyl-carrier protein reductase	membrane	unknown
YuaI	involved in reducing membrane fluidity	membrane	σ^W
NadE	NAD synthetase	energy	σ^B
BglH	phospho-beta-glucosidase	energy	CcpA
CitZ	citrate synthase	energy	CcpA
YwrO	similar to NAD(P)H oxidoreductase	energy	unknown
IolS	also/keto reductase	energy	IolR
YhdN	aldo/keto reductase specific for NADPH	energy	σ^B
NfrA	FMN-containing NADPH-linked nitro/flavin reductase	energy	Spx
RocA	3-hydroxy-1-pyrroline-5-carboxylate dehydrogenase	amino acids	RocR
TrmB	tRNA (m7G46) methyltransferase	tRNA modification	unknown
RpsB	ribosomal protein S2	translation	unknown
YvlB	unknown	unknown	unknown

Table S2: MALDI-ToF-MS data of identified cytosolic marker proteins (2D gel-based approach)

protein ID	protein name	mass weight	pI	peptide count	protein score		protein score C.I. %
AzoR2	azoreductase	23257	5.26	7	117		100
BglH	phospho-beta-glucosidase	53255	5.13	13	287		100
CitZ	citrate synthase	41702	5.55	16	444		100
ClpP	ATP-dependent Clp protease proteolytic subunit	21668	5.19	12	353		100
DltA	D-alanyl-D-alanine carrier protein ligase	55773	5.10	13	276		100
Dps	DNA-protecting protein, ferritin	16583	4.64	8	168		100
FosB	bacillithiol-S-transferase	17161	6.14	4	754	*	-
IolS	aldo/keto reductase	35146	5.50	16	280		100
LiaH	modulator of LiaIHGFSR operon expression	25682	6.20	13	112		100
NadE	NAD synthetase	30376	5.07	16	459		100
NfrA	FMN-containing NADPH-linked nitro/flavin reductase	28302	5.73	20	9602	*	-
PspA	phage shock protein A	25125	5.87	11	91		100
RacX	amino acid racemase	25270	5.46	3	73		100
RocX	3-hydroxy-1-pyrroline-5-carboxylate dehydrogenase	56284	5.58	52	12601	*	-
RpsB	ribosomal protein S2	27950	6.27	16	279		100
Spo0M	sporulation-control gene	29714	4.26	63	25783	*	-
SpoVG	negative effector of sporulation	10886	5.25	10	348		100
TrmB	tRNA (guanine-N(7)-)-methyltransferase	24488	6.32	7	53		98
YceC	similar to tellurium resistance protein	21810	5.46	14	224		100
YceH	unknown	41646	5.90	13	263		100
YdaG	general stress protein	15867	5.33	5	100		100
YdbD	manganese-containing catalase	30238	5.06	10	103		100
YfhM	similar to epoxide hydrolase	32737	6.07	20	7499	*	-
YhdN	aldo/keto reductase specific for NADPH	37289	4.96	10	132		100
YjdA	similar to 3-ketoacyl-acyl-carrier protein reductase	27432	5.74	5	55		99
YoxD	similar to 3-oxoacyl-acyl-carrier protein reductase	25283	5.48	20	434		100
YqiG	similar to NADH-dependent flavin oxidoreductase	40780	5.34	19	325		100
YthP	similar to ABC transporter	26490	5.39	5	195		100
YtrE	similar to ABC transporter	25444	5.99	11	241		100
YtxH	general stress protein	16675	5.30	5	131		100
YuaI	involved in reducing membrane fluidity	19830	5.31	7	167		100
YvlB	unknown	41056	5.50	15	121		100
YwrO	similar to NAD(P)H oxidoreductase	19942	5.33	7	166		100

* Identification was carried out using a Synapt G2S HDMS mass spectrometer (see SI Appendix, Experimental Details)

Table S3: Marker proteins induced in the membrane proteome

ID	protein function	pathway	category	repressor	activator
PtkA	protein tyrosine kinase involved in biofilm formation	antibiotic stress	stress response	AbrB	
YaaN	similar to toxic cation resistance protein	detoxication	stress response		σ^W
YfhM	similar to epoxide hydrolase	detoxication, sigma b dependent, phosphate starvation	stress response		σ^W/σ^B
RsbW	anti-sigma factor	general stress response sigma b	stress response		σ^B
PcrA	ATP-dependent DNA helicase	mismatch repair, nucleotide excision repair	stress response	LexA	
ClpX	ATP-dependent Clp protease ATP-binding subunit	heat shock	stress response	CtsR	
HslU	ATP-dependent protease ATP-binding subunit	heat shock	stress response	CodY	
DnaK	class I heat-shock protein	heat shock	stress response	HrcA	
LonA	class III heat-shock ATP-dependent Lon protease	heat shock	stress response	CtsR	
YciC	putative metallochaperone with NTPase activity/probably part of a low-affinity pathway of zinc transport	chaperone/zinc transport	stress response	Zur	
EngD	GTP-dependent nucleic acid-binding protein	competence	stress response		ComK
NucA	endonuclease	competence	stress response		ComK
DegS	two-component sensor histidine kinase	competence	stress response		
KinD	two-component sensor histidine kinase	sporulation	stress response		
SpoIVA	required for proper spore cortex formation and coat assembly	sporulation	stress response		σ^E
YlbC	unknown	sporulation	stress response		
McsB	protein arginine kinase	protein modification	stress response		
SrfAA	surfactin synthetase	antibiotic production	stress response	Abh, CodY, Spx	ComA, PerR
SrfAB	surfactin synthetase	antibiotic production	stress response	Abh, CodY, Spx	ComA, PerR
SrfAC	surfactin synthetase	antibiotic production	stress response	Abh, CodY, Spx	ComA, PerR
YsdB	unknown	control of SigW activity, survival of heat stress	cell envelope		σ^B/σ^W
YacL	unknown	survival of salt and ethanol stresses	cell envelope		σ^B/σ^M
YpuA	unknown	unknown	cell envelope		σ^M
YobJ	unknown	unknown	cell envelope		σ^W
YteJ	unknown	unknown	cell envelope		σ^W
BioD	dethiobiotin synthetase	biotin metabolism	membrane	BirA	
BioI	cytochrome P450 enzyme	biotin metabolism, detoxication	membrane	BirA	
AcpA	acyl carrier protein	fatty acid biosynthesis	membrane	FapR	
FabG	beta-ketoacyl-acyl carrier protein reductase	fatty acid biosynthesis	membrane	FapR	

ID	protein function	pathway	category	repressor	activator
PlsX	involved in fatty acid/phospholipid synthesis	fatty acid biosynthesis	membrane	FapR	
YhfT	similar to long-chain fatty-acid-CoA ligase	fatty acid biosynthesis	membrane		
FadE	acyl-CoA dehydrogenase	fatty acid biosynthesis	membrane	CcpA, FadE	SdpR
GlpD	glycerol-3-phosphate dehydrogenase	glycerophospholipid metabolism	membrane	CcpA	AbrB, GlpP
FloT	similar to flotillin 1, orchestration of physiological processes in lipid microdomains	control of membrane fluidity	membrane		
DynA	dynamin-like protein	membrane fusion	membrane		
DltB	D-alanine esterification of lipoteichoic acid and wall teichoic acid/D-alanyl transfer from Dcp to undecaprenol-phosphate	lipoteichoic acid biosynthesis	cell wall	Spo0A, stringent response	$\sigma^M/\sigma^X/\sigma^D$, YvrHb
DltD	D-alanine transfer from undecaprenol-phosphate to the poly(glycerophosphate) chain of LTA	lipoteichoic acid biosynthesis	cell wall	Spo0A, stringent response	$\sigma^M/\sigma^X/\sigma^D$, YvrHb
Ddl	D-alanyl-D-alanine ligase A	peptidoglycan biosynthesis	cell wall		σ^M
MreB	cell shape-determining protein	peptidoglycan biosynthesis	cell wall		σ^M
Mbl	MreB-like protein	peptidoglycan biosynthesis	cell wall	stringent response	σ^E
MurAB	UDP-N-acetylglucosamine 1-carboxyvinyltransferase	peptidoglycan biosynthesis	cell wall		
MurAA	UDP-N-acetylglucosamine 1-carboxyvinyltransferase	peptidoglycan biosynthesis	cell wall		
MurG	UDP-N-acetylglucosamine-N-acetylmuramyl-(pentapeptide)pyrophosphoryl-undecaprenol N-acetylglucosamine transferase	peptidoglycan biosynthesis	cell wall		
LytA	involved in the secretion of major autolysin LytC (amidase)	lysis and remodeling of peptidoglycan	cell wall	SlrR	σ^D, YvrHb
YycH	negative effector of WalK	control of cell wall metabolism	cell wall		
GdpP	cyclic di-AMP phosphodiesterase	cell wall homeostasis	cell wall		
YbbP	maybe involved in the synthesis of c-di-AMP in vegetative cells	cell wall homeostasis	cell wall		
FtsA	membrane anchor of FtsZ	septum formation	cell division		σ^H, WalR
YydI	ABC transporter (ATP-binding protein)	antibiotic transport system	transporter	AbrB, Rok	
YybJ	similar to ABC transporter (ATP-binding protein)	antibiotic transport system, iorganic ion transport	transporter		
YdbJ	similar to ABC transporter (ATP-binding protein)	antibiotic transport system, multidrug transporter	transporter		
YutK	similar to Na^+/nucleoside cotransporter	concentrative nucleoside transporter	transporter		
OpuAA	glycine betaine ABC transporter	osmoprotectant transport system, choline transport	transporter		
OpuCC	glycine betaine/carnitine/choline ABC transporter	osmoprotectant transport system, choline transport	transporter		
OpuBA	choline ABC transporter (ATP-binding protein)	osmoprotectant transport system, choline transport	transporter		
DppE	dipeptide ABC transporter	peptide transport	transporter	CodY	
OppD	oligopeptide ABC transporter (ATP-binding protein)	peptide transport	transporter	ScoC	TnrA

ID	protein function	pathway	category	repressor	activator
SufC	similar to ABC transporter, iron metabolism (ATP-binding protein)	transport	transporter		
ThiV	putative HMP/thiamine permease	amino acid/sugar metabolism	transporter	Thi-box	Thi-box
YlaG	GTPase	signal transduction	protein secretion	stringent response	
SecA	translocase binding subunit	protein secretion	protein secretion		
AtpC	ATP synthase	oxidative phosphorylation	energy metabolism	stringent response	
QoxC	cytochrome aa3 quinol oxidase (subunit III)	oxidative phosphorylation	energy metabolism	stringent response	
HemL	glutamate-1-semialdehyde 2,1-aminotransferase	porphyrin biosynthesis	energy metabolism	PerR	
SufB	synthesis of Fe-S-clusters	iron metabolism	energy metabolism		
ResE	two-component sensor histidine kinase	regulation of electron transport	energy metabolism	CcpA	PhoP, ResD
NadA	quinolinate synthetase	nicotineamide and nicotinate metabolism	energy metabolism	NadR	
NadB	L-aspartate oxidase	nicotineamide and nicotinate metabolism	energy metabolism	NadR	
NadF	probable inorganic polyphosphate/ATP-NAD kinase 2	nicotineamide and nicotinate metabolism	energy metabolism		
PncB	nicotinate phosphoribosyltransferase	nicotineamide and nicotinate metabolism	energy metabolism		
ThiC	biosynthesis of the pyrimidine moiety of thiamin	amino acid/sugar metabolism	energy metabolism	Thi-box	Thi-box
SucC	succinyl-CoA synthetase (beta subunit)	TCA cycle	energy metabolism	CcpA	
CitB	aconitate hydratase	TCA cycle	energy metabolism	CcpC, CodY, FrsA	
Icd	isocitrate dehydrogenase	TCA cycle	energy metabolism	CcpA, CcpC	
PycA	pyruvate carboxylase	TCA cycle	energy metabolism		stringent response
AckA	acetate kinase	pyruvate metabolism	energy metabolism		CcpA, CodY
Tkt	transketolase	glycolysis	energy metabolism	Spo0A	
Pgk	phosphoglycerate kinase	glycolysis	energy metabolism	CggR	
Pyk	pyruvate kinase	glycolysis	energy metabolism		
GapA	glyceraldehyde-3-phosphate dehydrogenase	glycolysis	energy metabolism	CggR	
Tal	putative transaldolase	pentose phosphate pathway	energy metabolism		
PtsI	phosphotransferase system (PTS) enzyme I	PTS	energy metabolism	stringent response	GlcT
FrlB	similar to glutamine-fructose-6-phosphate transaminase	carbohydrate & nitrogen metabolism	energy metabolism	CodY, FlrR	
FrlO	similar to multiple sugar-binding protein	carbohydrate & nitrogen metabolism	energy metabolism	CodY, FrlR	
YoaC	similar to xylulokinase	carbohydrate metabolism	energy metabolism	S-box	S-box
BdhA	acetoin reductase/2,3-butanediol dehydrogenase	carbohydrate metabolism	energy metabolism		AbrB
YqfL	modulator of CcpN activity	carbohydrate metabolism	energy metabolism		
GndA	NADP-dependent phosphogluconate dehydrogenase	carbohydrate metabolism	energy metabolism		
LutB	lactate catabolic enzyme	carbohydrate metabolism	energy metabolism	LutR	

ID	protein function	pathway	category	repressor	activator
YitJ	probable 5,10-methylenetetrahydrofolate reductase (NADP)	unknown	energy metabolism	S-box	S-box
PurA	adenylosuccinate synthetase	purine	nucleotide synthesis	PurR, G-box	G-box
PurB	adenylosuccinate lyase	purine	nucleotide synthesis	PurR, G-box	G-box
PurC	phosphoribosylaminoimidazole succinocarboxamide synthetase	purine	nucleotide synthesis	PurR, G-box	G-box
PurD	phosphoribosylglycinamide synthetase	purine	nucleotide synthesis	PurR, G-box	G-box
PurF	glutamine phosphoribosylpyrophosphate amidotransferase	purine	nucleotide synthesis	PurR, G-box	G-box
PurH	phosphoribosylaminoimidazole carboxy formyl formyltransferase and inosine-monophosphate cyclohydrolase	purine	nucleotide synthesis	PurR, G-box	G-box
PurK	phosphoribosylaminoimidazole carboxylase II	purine	nucleotide synthesis	PurR, G-box	G-box
PurL	phosphoribosylformylglycinamidine synthetase II	purine	nucleotide synthesis	PurR, G-box	G-box
Xpt	xanthine phosphoribosyltransferase	purine	nucleotide synthesis	PurR, G-box	G-box
MtnN	methylthioadenosine/S-adenosylhomocysteine nucleosidase	purine	nucleotide synthesis	Spx	CymR
PyrAB	carbamoyl-phosphate synthetase	pyrimidine	nucleotide synthesis		PyrR
PyrE	orotate phosphoribosyltransferase	pyrimidine	nucleotide synthesis		PyrR
PyrH	uridylate kinase	pyrimidine	nucleotide synthesis		PyrR
PyrR	transcriptional attenuator and uracil phosphoribosyltransferase activity	pyrimidine	nucleotide synthesis		PyrR
CarA	carbamoyl-phosphate transferase-arginine	Ala, Asp, Glu	amino acids		AhrC
CarB	carbamoyl-phosphate transferase-arginine	Ala, Asp, Glu	amino acids		AhrC
GltA	glutamate synthase (large subunit)	Ala, Asp, Glu	amino acids	GltC	FsrA, TnrA
AsnB	asparagine synthetase	Ala, Asp, Glu	amino acids		
GudB	glutamate dehydrogenase	Ala, Asp, Glu, Arg, Pro	amino acids		
ArgH	argininosuccinate lyase	Ala, Asp, Glu, Arg, Pro	amino acids		AhrC
ArgJ	ornithine acetyltransferase and amino-acid acetyltransferase	Ala, Asp, Glu, Arg, Pro	amino acids		AhrC
YhdR	similar to aspartate aminotransferase	Ala, Asp, Glu, Arg, Pro, Cys, Met, Phe, Tyr, Trp	amino acids		
AlaT	alanine transaminase	Arg, Pro, Lys	amino acids		
MetC	similar to cystathionine beta-lyase	Cys, Met	amino acids	S-box	S-box
MetE	cobalamin-independent methionine synthase	Cys, Met	amino acids	S-box	S-box
MetK	S-adenosylmethionine synthetase	Met, SAM	amino acids	S-box	S-box
MtnK	methylthioribose kinase	Cys, Met	amino acids	S-box	S-box
YxjG	putative methionine synthase	met	amino acids	S-box	S-box
CysJ	similar to sulfite reductase	sulfur metabolism	amino acids	CysL	
Sat	sulfate adenylyltransferase	sulfur metabolism	amino acids	S-box	S-box
ThiO	glycine oxidase	Gly, Ala, Val, Pro	amino acids	Thi-box	Thi-box
HisA	phosphoribosylformimino-5-aminoimidazole carboxamide ribotide isomerase	His	amino acids	T-box	T-box

ID	protein function	pathway	category	repressor	activator
LysC	aspartokinase II alpha subunit (aa 1-408) and beta subunit (aa 246-408)	Lys, Cys, Met, Gly, Ser, Thr	amino acids		
AroA	3-deoxy-D-arabino-heptulosonate 7-phosphate synthase and chorismate mutase-isozyme 3	Phe, Tyr, Trp	amino acids		
AroB	3-dehydroquinate synthase	Phe, Tyr, Trp	amino acids		
AroE	5-enolpyruvoylshikimate-3-phosphate synthase	Phe, Tyr, Trp	amino acids		
AroF	chorismate synthase	Phe, Tyr, Trp	amino acids		
ProA	gamma-glutamyl phosphate reductase	Arg, Pro	amino acids	T-box	T-box
LeuA	2-isopropylmalate synthase	Val, Leu, Ile	amino acids	T-box, CodY, CcpA, TnrA	T-box
LeuC	3-isopropylmalate dehydratase (large subunit)	Val, Leu, Ile	amino acids	T-box, CodY, CcpA, TnrA	T-box
LeuD	3-isopropylmalate dehydratase (small subunit)	Val, Leu, Ile	amino acids	T-box, CodY, CcpA, TnrA	T-box
IlvB	acetolactate synthase catalytic subunit	Val, Leu, Ile	amino acids	T-box, CodY, CcpA, TnrA	T-box
IlvD	dihydroxy-acid dehydratase	Val, Leu, Ile	amino acids	T-box, CodY, CcpA, TnrA	T-box
YwaA	similar to branched-chain amino acid aminotransferase	Val, Leu, Ile	amino acids		
RelA	ppGpp hydrolase/synthase	stringent response, amino acid starvation	amino acids		
YdbR	similar to ATP-dependent RNA helicase	transcription regulation	transcription		
GlpP	transcription antiterminator	transcription regulation	transcription		GlpP
Rho	transcriptional terminator Rho	transcription regulation	transcription		
TufA	elongation factor TU	elongation	translation	stringent response	
FusA	elongation factor G	elongation	translation	stringent response	
RplA	ribosomal protein L1	ribosomal proteins	translation	stringent response	
YydA	similar to pseudouridine methyltransferase	rRNA maturation	translation	DnaA	
YmcB	tRNA methylthiotransferase	tRNA maturation	translation		
ProS	prolyl-tRNA synthetase	tRNA synthetase (Pro)	translation		
ThrS	threonyl-tRNA synthetase	tRNA synthetase (Thr)	translation	T-box	T-box
ThrZ	threonyl-tRNA synthetase	tRNA synthetase (Thr)	translation	T-box	T-box
LysS	lysyl-tRNA synthetase	tRNA synthetase (Lys)	translation		
HisS	histidyl-tRNA synthetase	tRNA synthetase (His)	translation	T-box	T-box
GatA	glutamyl-tRNA(Gln) amidotransferase	tRNA transferase (Glu)	translation		

ID	protein function	pathway	category	repressor	activator
GatB	glutamyl-tRNA(Gln) amidotransferase	tRNA transferase (Glu)	translation		
YebA	probable membrane protein	unknown	unknown		
YfhO	putative membrane protein	unknown	unknown		
YddK	unknown	unknown	unknown		
YgaO	unknown	unknown	unknown		
YydB	unknown	unknown	unknown		
YufK	unknown	unknown	unknown		
YjcH	unknown	unknown	unknown		
YjjA	unknown	unknown	unknown		
YjlC	unknown	unknown	unknown		
YqeG	unknown	unknown	unknown		

Table S4: ESI-MS data of the marker proteins identified in the membrane proteome

	control (replicate 1)			control (replicate 2)			MP196 (replicate 1)			MP196 (replicate 2)		
protein ID	**ratio**	**SD**	**peptides**	**ratio**	**SD**	**peptides**	**ratio**	**SD**	**peptides**	**ratio**	**SD**	**peptides**
O05249|yufK							1.71	0	2	2.21	0.15	2
O06491|gatA				1.4	0.14	4	14.35	8.69	9	10.78	14.49	4
O06745|yitJ	0.52	0.03	2	0.55	0.03	7	4.4	0.54	12	9.53	1.23	9
O07021|yvfW	1.71	0.18	2				10.03	1.31	5	16.02	5.6	4
O07587|yhdR							25.25	8.15	5	52.68	71.85	2
O07619|yhfT							23.06	2.96	2	38.66	12.71	4
O07631|typA				1.3	0.13	4	6.73	0.48	8	18.58	2.12	4
O30509|gatB				1.54	0.32	3	16.72	9.55	4	40.15	27.31	3
O31581|yfhM							21.9	1.78	3	30.97	2.39	2
O31582|yfhO				1.39	0.07	3	3.67	0.34	5	4.77	0.5	3
O31630|yjcH							5.66	0.59	3	5.2	0.97	3
O31632|yjcJ							10.16	1.13	2	24.1	26.22	2
O31663|mtnK	1.33	0.08	4	1.41	0.07	7	18.27	1.81	12	53.31	6.45	6
O31671|kinD							2.4	0.49	4	3.07	0.45	2
O31749|pyrH	0.82	0.03	2	0.93	0.04	2	8.06	1	5	12.27	0.4	2
O31755|proS							9.17	9.34	3	39.81	30.51	2
O31778|ymcB							27.39	20.03	3	68.55	4.23	2
O32028|mtnN	1.64	0.12	2				16.5	12.38	3	39.83	9.41	2
O32039|hisS				1.13	0.03	4	6.51	0.28	4	11.98	1.95	2
O32076|yuaG	1.4	0.16	15	1.41	0.09	13	13.26	1.29	28	13.47	1.56	18
O32090|yueK							3.13	0.32	4	5.68	0.81	5
O32115|yutK				0.7	0.05	2	1.31	0.01	2	1.73	0.36	6
O32156|yurO				0.79	0.07	2	2.45	0.2	8	4.33	0.06	3
O32157|yurP				0.81	0.1	3	19.31	9.97	4	45.29	4.68	2
O32162|yurU				1.19	0.08	2	23.31	1.96	6	62.73	3.09	3
O32176|yusJ							18.81	12.36	2	24.44	14.4	2
O32213|yvgQ							16.21	6.06	4	24.38	2.68	3
O32243|opuCC	1.27	0.07	6				2.93	0.05	3	3.54	0.07	3
O34394|yjjA							17.96	0.17	2	29.44	5.56	2
O34424|yteJ							3.7	0.46	2	4.06	0.55	4
O34580|pcrA	1.24	0.09	2	1.28	0.29	5	7.69	1.42	3	31.05	4.62	2
O34586|ylbC							2.18	0.31	2	2.63	0.35	3
O34633|yjlC							1.68	0.06	2	2.76	0.04	2
O34738|ykoE							1.34	0.12	4	1.8	0.13	2
O34764|sat							2.46	2.48	2	12.92	2.1	3
O34774|yobJ	0.81	0.12	4	0.86	0.1	7	5.78	0.47	7	6.44	0.79	5
O34788|ydjL				1.29	0.05	2	3.74	0.23	6	11.06	0.58	4
O34858|argH							7.99	0.94	4	28.52	5.81	4
O34861|yoaC							4.69	0.26	6	6.4	5.3	3
O34934|ppnK2							21.31	2.49	2	24.87	0.89	2
O35006|hisA							5.9	0.71	4	10.07	0.74	3
O54408|relA				1.02	0.06	9	4.64	0.53	8	12.12	1.05	3
P00497|purF	1.31	0.14	3				10.58	2.1	4	24.59	1.07	2
P08495|lysC				2.18	1.13	2	18.32	5.18	4	87.52	8.66	2
P08838|ptsI				0.97	0.09	7	2.45	0.1	4	10.28	0.93	5

	control (replicate 1)			control (replicate 2)			MP196 (replicate 1)			MP196 (replicate 2)		
protein ID	ratio	SD	peptides	ratio	SD	peptides	ratio	SD	peptides	ratio	SD	peptides
P09339|citB				0.79	0.19	3	3.36	0.63	3	7.72	1.22	9
P09124|gapA	1.28	0.12	7	1.21	0.09	6	31.91	5.15	5	71.4	40.82	6
P12039|purD	1.4	0.1	4	1.7	0.04	2	19.18	5.95	4	30.92	2.22	8
P12042|purL	1.29	0.05	3	1.27	0.02	8	26.81	2.12	11	40.4	1.84	9
P12045|purK							7.39	1.57	6	11.22	0.81	3
P12046|purC	1.62	0.13	2	1.38	0.26	3	20.33	9.8	7	43.25	8.5	3
P12047|purB				1.07	0.09	3	5.86	0.11	6	14.41	3.35	7
P12048|purH	1.82	0.25	3	1.59	0.16	5	20.81	4.22	6	73.17	48.09	5
P12667|nucA							0.72	0.06	3	1.11	0.41	2
P13799|degS	1.11	0.04	2				11.66	0.92	6	18.85	1.21	3
P17820|dnaK				1.7	0.04	7	40.41	4.5	6	58.99	31.1	10
P17904|rsbW							20.96	4.87	2	40.23	1.16	2
P18185|carB	1.28	0.18	2	1.19	0.04	4	9.55	0.88	5	28.6	3.26	10
P18255|thrS				0.66	0.11	6	4.11	0.26	9	21.44	9.09	7
P18256|thrZ				0.91	0.03	7	10.98	1.1	7	24.32	3.32	7
P19669|tal	1.06	0.29	2				2.07	0.17	4	4.28	0.28	3
P19670|murAB							18.25	2.28	2	14.27	18.88	2
P20691|aroE							28.16	2.08	4	35.76	38.25	2
P24136|oppD							3.15	0.33	2	4.01	0.06	3
P25972|pyrE	1.09	0.19	2				9.46	0.82	2	11.65	1.12	2
P25994|pyrAB				0.66	0.03	10	3.28	0.41	13	7.01	0.57	17
P26906|dppE				0.78	0.03	3	4.83	0.01	2	5.38	0.75	4
P27206|srfAA	0.37	0.07	12	0.38	0.05	31	1.99	0.49	37	3.86	0.98	37
P28264|ftsA							10.64	1.52	2	15.15	0.48	2
P28366|secA	1.07	0.11	6	1.04	0.04	17	10.56	0.89	18	16.05	0.77	15
P29726|purA	0.84	0.09	6	0.92	0.12	4	6.25	1.57	13	8.39	2.31	9
P30300|glpP							3.25	0.15	2	4.66	1.19	2
P30949|hemL							7.88	0.33	5	8.33	5.49	4
P31102|aroB	1.7	0.12	4	1.81	0.23	7	20.1	8.99	8	92.54	21.03	2
P31104|aroF				2.12	0.11	2	16.64	0.7	3	45.26	42.15	2
P31847|ypuA				0.86	0.1	4	8.65	1.54	3	10.55	1.32	2
P33166|tuf	1.33	0.06	11	1.35	0.07	12	14.29	2.68	14	32.7	20.2	11
P34958|qoxC				0.72	0.2	5	1.95	0.13	4	2.14	0.05	2
P35149|spoIVA							1.77	0.11	2	0.87	0.13	3
P35164|resE				0.86	0.06	4	2.86	0.66	7	4.04	1.09	5
P36838|carA	1.12	0	2				4.93	0.34	5	13.23	3.95	6
P36843|argJ							61.37	6.39	2	118.98	14.3	2
P37484|yybT				0.96	0.08	2	2.53	0.26	5	3.3	0.29	6
P37494|yybJ	0.67	0.02	4				3.32	0.18	4	3.42	1.04	2
P37518|engD				3.22	0.29	4	13.05	5.67	6	21.23	13.14	4
P37535|yaaN				1.29	0.04	2	19.02	3	6	30.73	9.04	4
P37570|yacI							7.15	0.55	2	12.29	2.4	2
P37585|murG				0.8	0.05	4	4.98	1.05	2	8.78	1.66	2
P37812|atpC							2.78	0.07	2	2.85	0.26	3
P37877|ackA							65.81	37.52	4	102.55	95.95	3
P37945|lonA	0.92	0.16	2	0.97	0.07	7	5.21	0.35	8	12.03	1.84	6
P38032|nadB							6.57	2.71	6	14.48	1.14	6

	control (replicate 1)			control (replicate 2)			MP196 (replicate 1)			MP196 (replicate 2)		
protein ID	ratio	SD	peptides	ratio	SD	peptides	ratio	SD	peptides	ratio	SD	peptides
P39580|dltB				0.7	0.01	2	4.48	0.19	3	5.36	0.04	2
P39126|icd	1.06	0.27	6	1.14	0.16	7	5.38	0.34	10	10.55	1.91	12
P39578|dltD				1.03	0.08	4	4.79	0.24	7	5.42	0.85	5
P39765|pyrR	1.38	0.11	3	1.24	0.3	2	9.22	4.19	5	16.67	1.31	2
P39778|hslU				0.92	0.21	2	4	0.94	2	6.23	0.06	2
P39812|gltA				1.07	0.06	8	6.42	0.67	15	15.77	1.12	8
P39821|proA							18.31	2.45	6	39.4	1.47	2
P39912|aroA	1.08	0.23	5	1.15	0.19	6	8.08	1.52	10	17.58	1.26	6
P40924|pgk	1.97	0.33	3				15.65	1.1	6	32.31	6.73	7
P42085|xpt	1.56	0.01	2	1.57	0	2	20.72	5.09	3	52.97	2.28	2
P42318|yxjG							6.22	2.51	5	15.56	10.04	3
P45694|tkt				0.96	0.06	2	3.84	0.89	5	9.49	5.62	4
P45740|thiC							10.48	1.83	5	17.86	4.36	4
P46920|opuAA	1.07	0.07	4	0.93	0.04	2	5.5	0.39	10	8.87	1.38	4
P50735|gudB	0.52	0.09	3	0.62	0.03	2	5.24	0.15	6	8	0.58	7
P50866|clpX	0.97	0.02	2	1.04	0.09	5	7.62	3.94	4	20.36	0.75	2
P51785|ilvD				0.62	0.51	3	5.46	0.56	5	19.38	2.31	3
P51831|fabG							6.56	1.8	5	11.35	6.31	3
P53554|bioI							12.5	1.01	6	27.23	0.72	3
P53558|bioD							5.79	1.53	5	4.15	2.67	2
P54159|ypbR				0.87	0	2	3.38	0.14	2	6.88	1.53	2
P54419|metK	1.25	0.02	2	1.24	0.06	2	19.29	2.16	5	23.24	10.18	6
P54420|asnB	0.87	0.06	3	0.84	0.05	13	5.32	0.31	15	9.95	0.59	9
P54452|yqeG							1.77	0.06	2	2.45	0.71	2
P54470|yqfL							7.9	0.05	2	13.59	0.24	2
P71018|plsX				0.67	0.04	6	3.95	0.77	6	7.23	0.18	2
P71068|yukA				0.48	0.05	5	2.11	0.6	6	2.92	1.16	7
P80643|acpA							7.6	1.07	3	10.09	2.91	2
P80858|leuC							33.35	6.13	5	55.04	10.45	3
P80859|yqjI							7.59	1.39	3	6.35	7.61	2
P80866|yurY				1.39	0.25	4	7.25	2.37	3	10.56	3.24	3
P80868|fusA	1.45	0.6	4	1.17	0.07	10	12.36	2.15	11	32.33	2.28	6
P80877|metE	1	0.21	10	1.18	0.05	20	26.19	3.04	31	102.19	10.78	18
P80885|pyk				1.91	0.11	3	11.4	10.5	2	32.48	8.78	4
P80886|sucC	1.15	0.15	3	1.14	0.11	9	14.72	1.08	11	36.83	14.83	7
P94400|yciC				1.41	0.05	2	7.04	0.48	7	27.2	3.92	4
P94476|yebA							1.48	0.16	2	2.03	0.04	2
P94520|ysdB							2.69	0.1	2	3.12	0.4	4
P96614|ydbR	0.83	0.15	3	0.77	0.05	9	4.3	2.53	9	5.91	2.13	7
P96648|yddK							0.27	0.03	2	0.77	0.06	3
P96716|ywqD							5.99	5.7	2	5.68	6.7	2
P97029|ygaO							1.8	0.15	2	2.04	0.2	3
Q01465|mreB	0.96	0.09	3	1.04	0.07	6	16.42	2.82	5	22.72	1.66	6
Q02112|lytA							0.44	0.02	3	0.67	0.14	3
Q03222|rho							3.32	0.01	2	3.41	0.05	3
Q04747|srfAB	0.35	0.08	14	0.44	0.06	42	2.19	0.26	44	3.98	0.45	35
Q06754|yacL				1.03	0.03	2	4.48	0.12	2	4.8	0.78	2

	control (replicate 1)			control (replicate 2)			MP196 (replicate 1)			MP196 (replicate 2)		
protein ID	**ratio**	**SD**	**peptides**	**ratio**	**SD**	**peptides**	**ratio**	**SD**	**peptides**	**ratio**	**SD**	**peptides**
Q45593|yydI							3.39	0.78	3	4.31	1.16	2
Q06797|rplA				0.98	0.36	2	2.41	0.52	2	4.12	0.2	2
Q45589|ybbP				0.71	0.15	2	2.26	0.37	5	2.78	0.62	4
Q45600|yydB							19.62	5.97	6	38.72	50.53	2
Q45601|yydA							1.26	0.05	2	2.65	0.69	2
Q794W0|yycH				0.94	0.1	3	2.29	0.26	7	3.12	0.27	7
Q795M6|alaT							4.35	1.08	4	9.29	0.37	2
Q9KWU4|pyc	1.17	0.01	2	1.08	0.05	9	10.42	1.04	17	23.43	1.85	16
Q9KWZ1|nadA							44.25	8.8	4	49.76	43.2	3

Table S5: Marker proteins of MP196 overlapping with markers of other cell envelope-targeting antibiotics - a comparison with the *B. subtilis* proteome response library (14,31). Non-overlapping proteins are not listed but included in the "total marker" count.

	MP196	vancomycin	bacitracin	mersacidin	nisin	gallidermin	gramicidin S	daptomycin	gramicidin A	valinomycin
general stress	YtxH									x
	GsiB						x			x
sporulation	Spo0M			x	x	x	x			
	SpoVG									x
cell envelope stress	YceC	x	x	x		x	x			x
	YceH					x	x		x	x
	LiaH		x	x	x	x	x	x		
	YtrE	x	x	x	x	x				
	DltA		x			x				
	RacX									x
	PspA				x	x	x	x	x	x
	YthP									
	YuaI									x
	YjdA						x			x
	YoxD	x					x		x	x
	YfhM						x			
	FosB						x			
energy	NadE				x	x			x	x
	BglH									x
	CitZ									x
	NfrA					x	x			x
	YwrO						x			
	YhdN									x
oxidative stress	YdbD						x			x
tRNA modification	TrmB			x	x	x				
translation	RpsB					x				
unknown	YvlB			x		x	x			
overlapping / total markers	35/35	3/5	4/8	6/12	6/8	12/21	14/17	2/8	4/5	16/20

Table S6: Ruthenium concentrations in subcellular fractions of cells treated with the ruthenocene-containing peptide derivative MP276.

	ruthenium per cell (pmol)		ruthenium per compartment volume* (pmol/µL)	
	control	MP276	control	MP276
cells	1.57×10^{-9}	1.45×10^{-7}	-	-
cytosol	2.59×10^{-9}	1.85×10^{-7}	0.65	46.29
membrane	1.85×10^{-9}	6.37×10^{-8}	20.61	709.41
cell wall	0	3.38×10^{-8}	0	41.93

vi) SI Figures

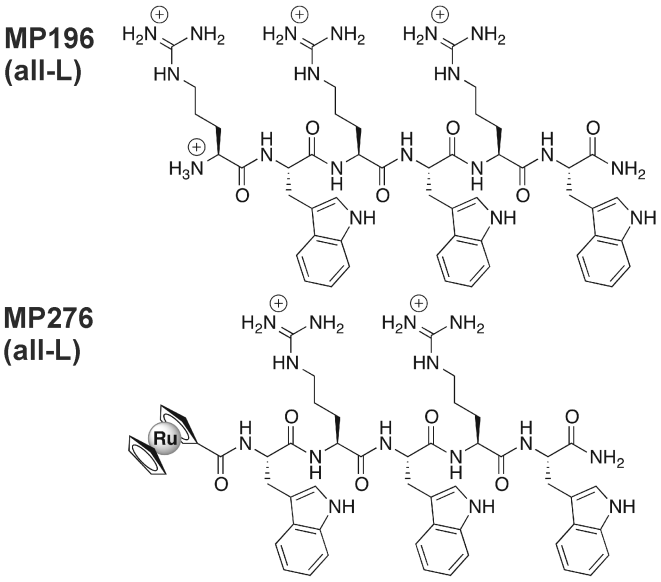

Figure S1: Chemical structures of MP196 and MP276.

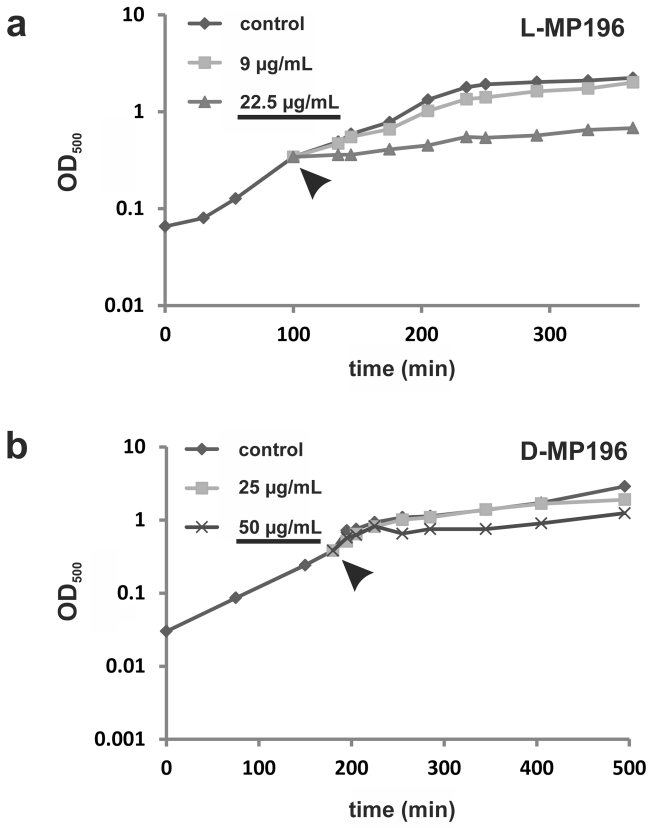

Figure S2: Growth of *B. subtilis* in chemically defined medium after treatment with MP196 **(a)** and D-MP196 **(b)**. Arrowheads indicate the time point of antibiotic addition during logarithmic growth. Peptide concentrations leading to ~50% growth inhibition in relation to the untreated controls were chosen for radioactive labeling and follow up experiments (chosen concentrations are underlined).

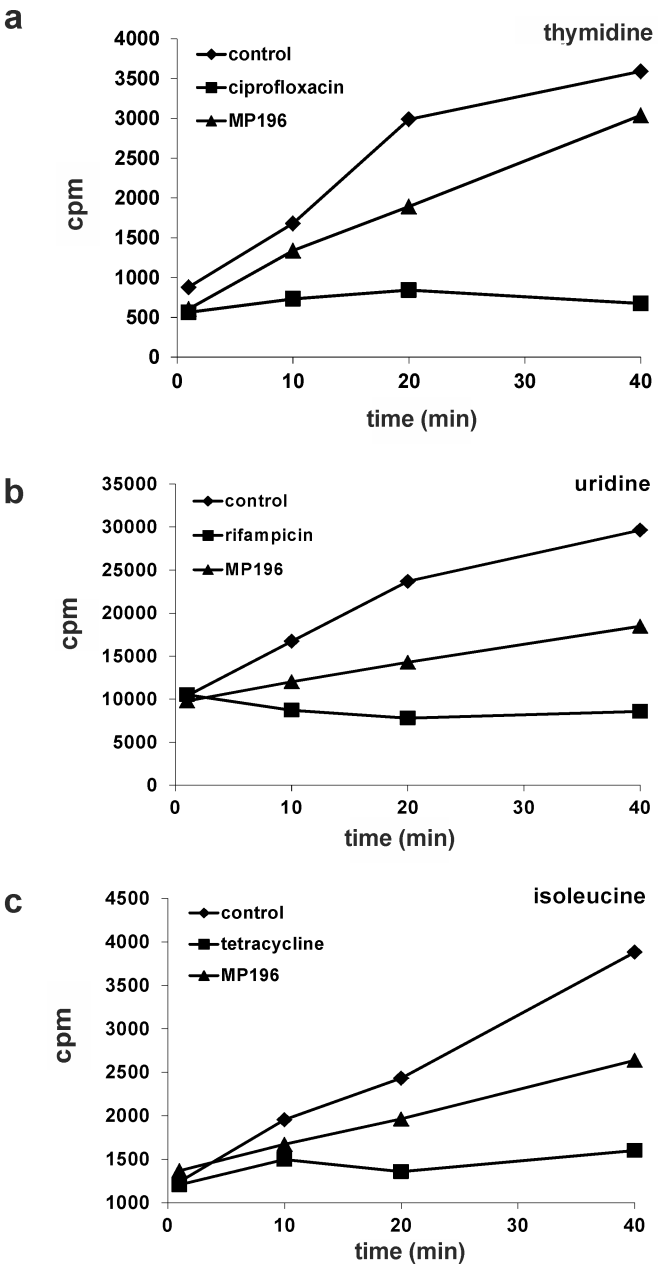

Figure S3: Incorporation of radioactively labeled precursor molecules by *Staphylococcus simulans* upon treatment with MP196 or pathway-specific inhibitors: **(a)** DNA precursor thymidine, **(b)** RNA precursor uridine, **(c)** protein precursor isoleucine.

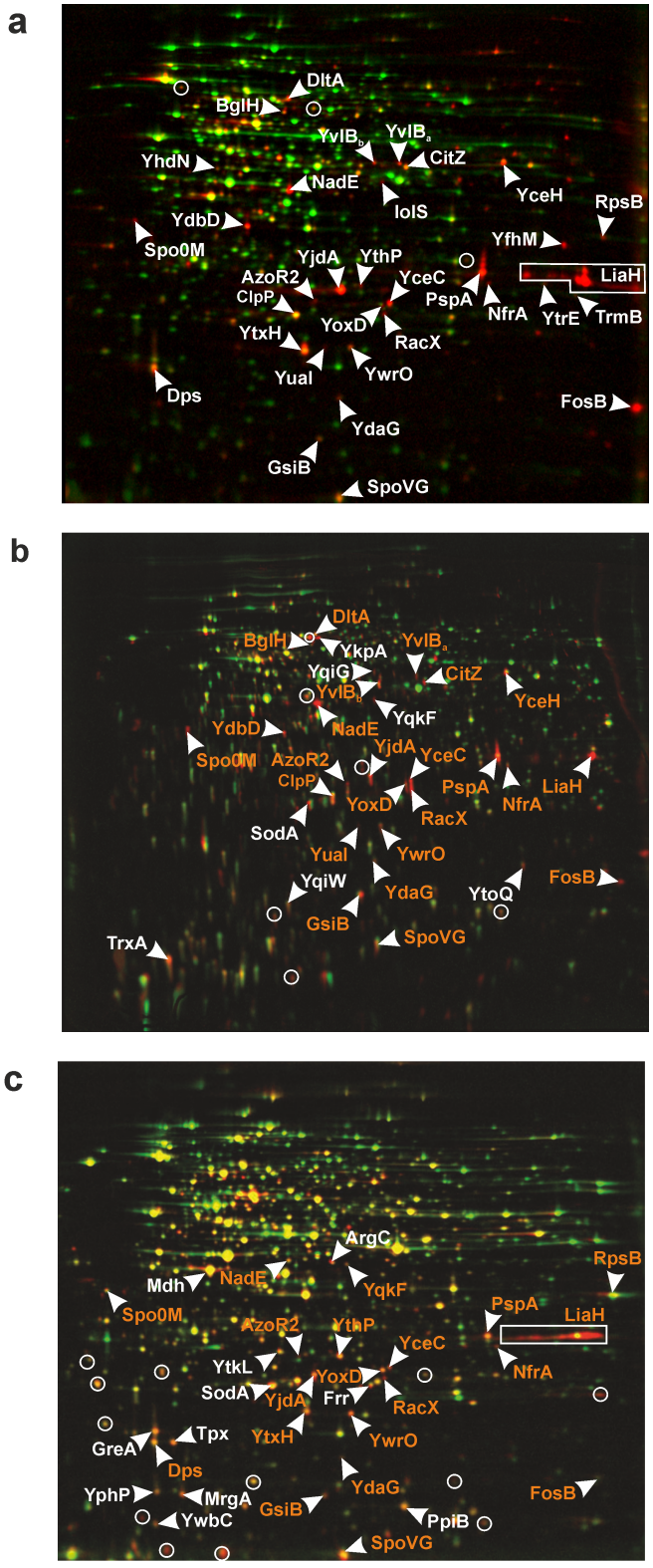

Figure S4: 2D gel-based proteome response of *B. subtilis* after treatment with MP196 **(a)** and D-MP196 **(b)**. Marker proteins upregulated in response to both peptides **(c)**. Overlapping proteins are labeled in orange. Unidentified proteins are circled.

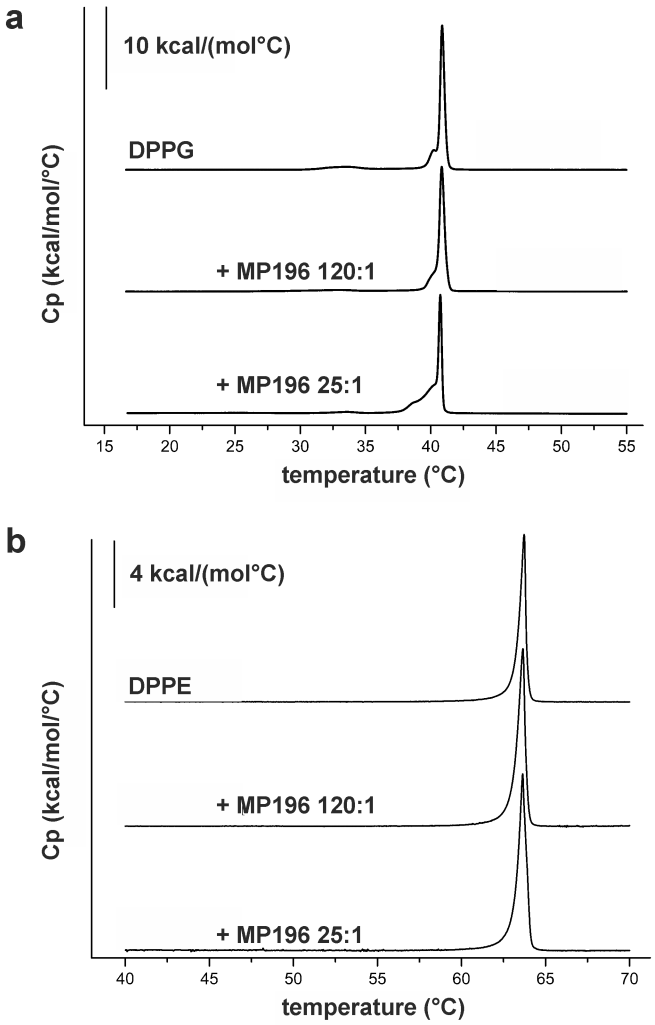

Figure S5: DSC thermograms of pure DPPG **(a)** and DPPE **(b)** incubated with MP196.

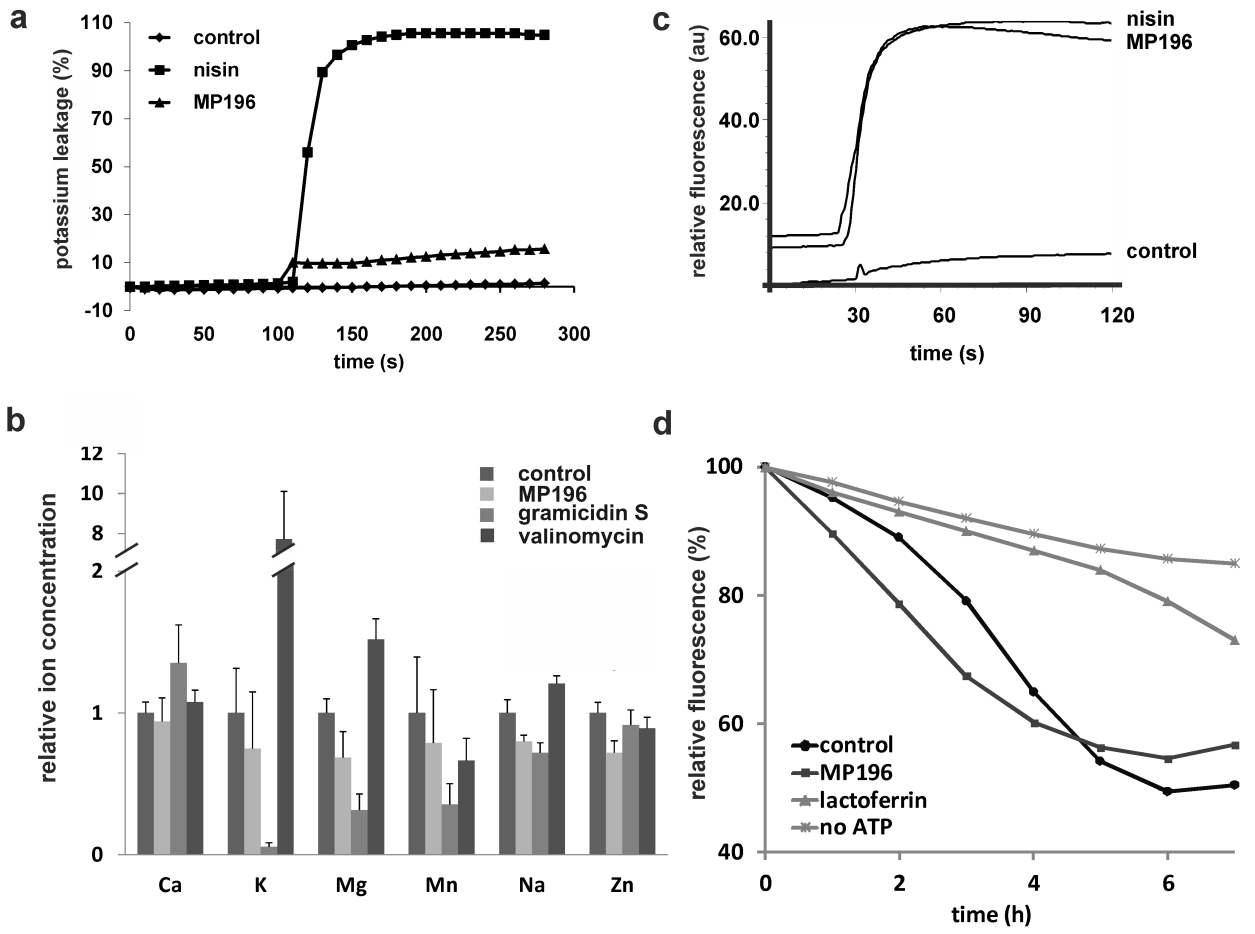

Figure S6: (a) Potassium release from whole *B. megaterium* cells. Values are given relative to positive control nisin, which forms pores. **(b)** Total ion profiles of *B. subtilis* stressed with valinomycin, gramicidin S, and MP196 in defined medium under physiological conditions. **(c)** $DiSC_35$-based depolarization measurements of *B. megaterium* treated with MP196 and nisin, a pore-forming lantibiotic serving as positive control. **(d)** H^+-ATPase activity of *M. flavus* inverted vesicles treated with lactoferrin and MP196. Proton pumping activity was measured by the pH-dependent absorbance change of acridine orange at 495 nm.

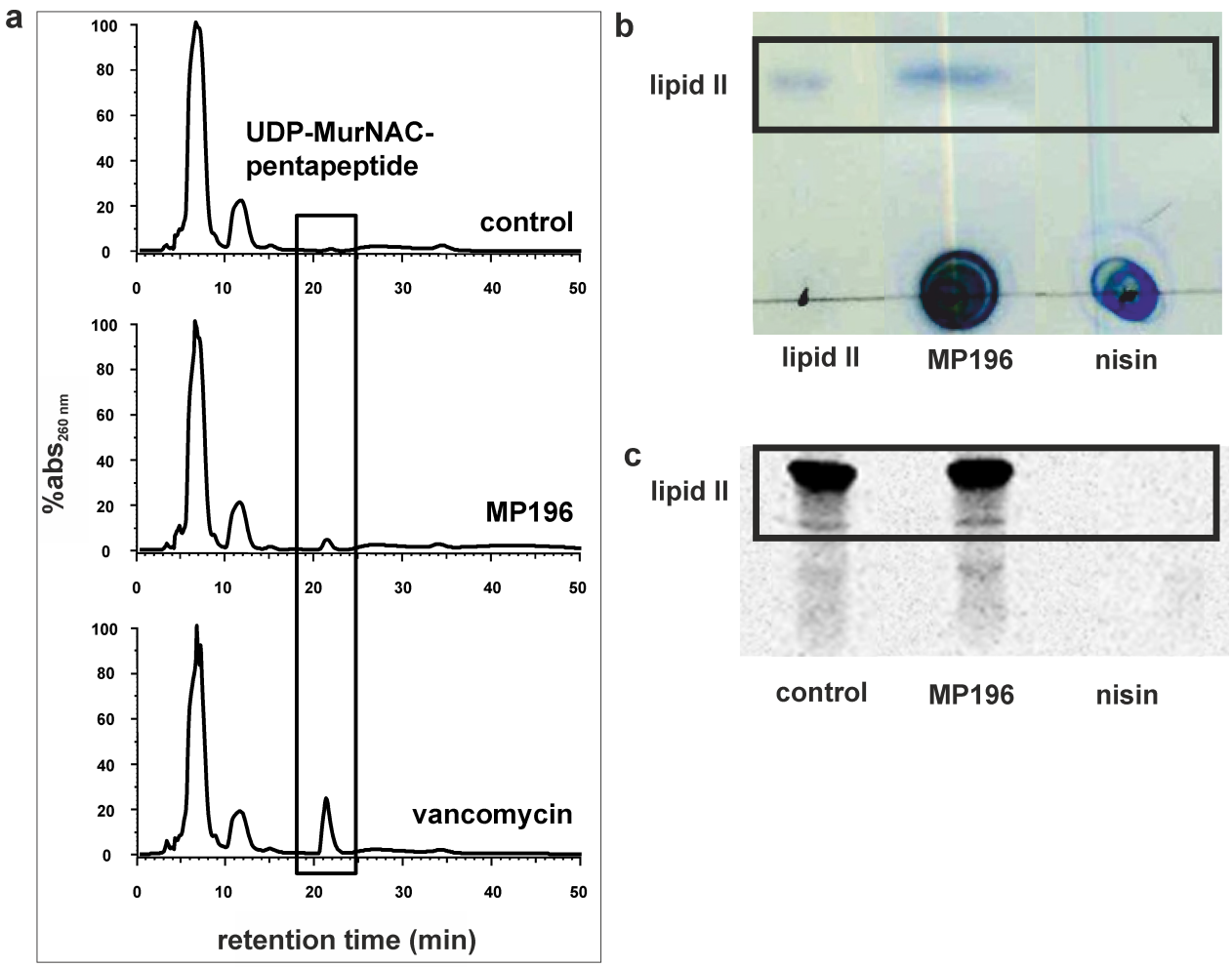

Figure S7: (a) HPLC chromatographs showing accumulation of the cell wall precursor UDP-MurNac pentapeptide by *S. aureus* cultures treated with MP196 and vancomycin. **(b)** TLC showing *in vitro* binding capability of MP196 and nisin to lipid II. **(c)** Thin layer chromatography (TLC) of radioactively labeled lipid II showing influence of MP196 and nisin on *in vitro* lipid II synthesis.

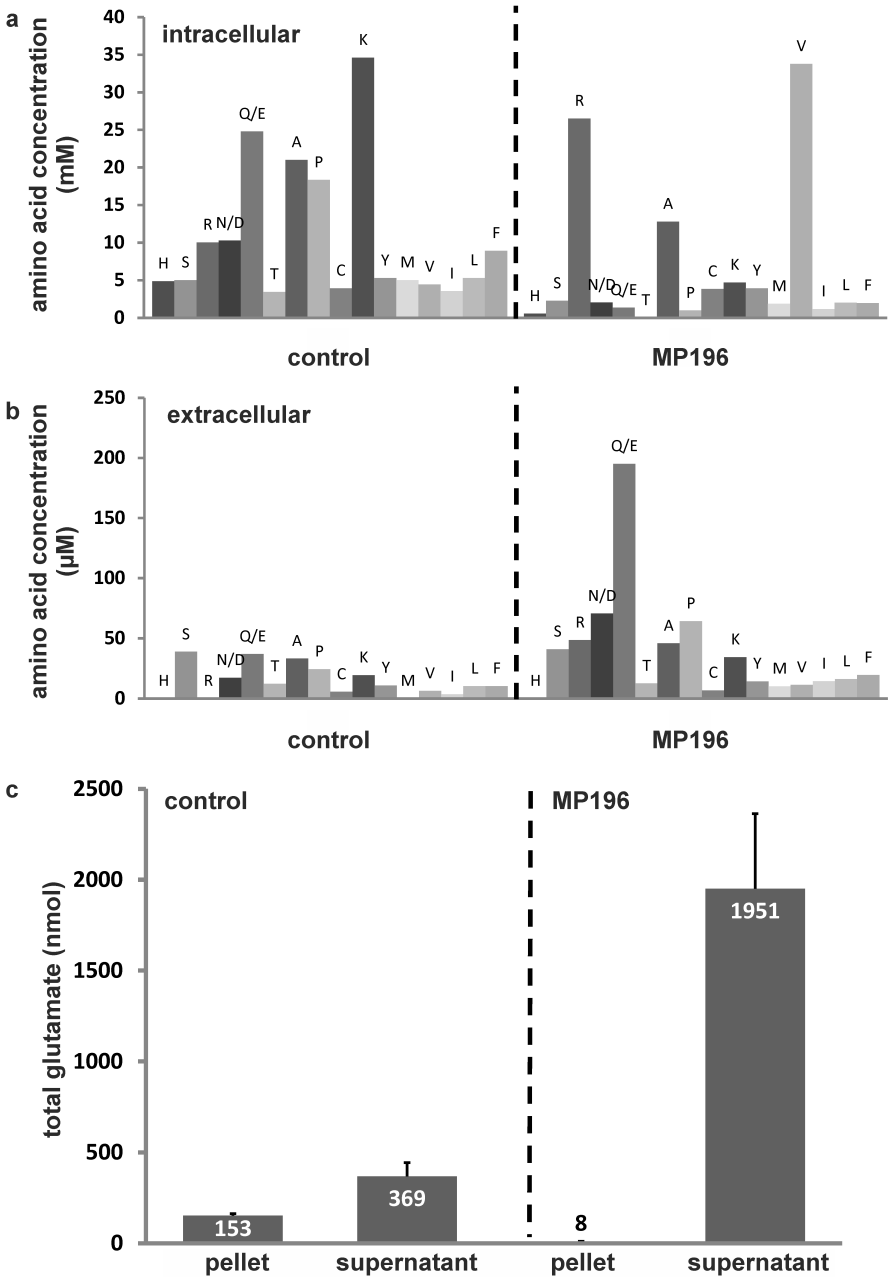

Figure S8: Free amino acid profiles of *B. subtilis* after MP196-treatment determined by HPLC: **(a)** intracellular amino acid concentrations **(b)** extracellular amino acid concentrations. Amino acids are written in one letter code in the order of elution time from the column. Glutamate and glutamine as well as aspartate and asparagine are not separated and appear as one peak. Tryptophan was not quantified here. **(c)** Total glutamate determination: *B. subtilis* were harvested from 10 ml of an exponentially growing culture. The cells were resuspended in AAA buffer and treated with MP196 or left untreated. After 15 min, cells were harvested by centrifugation and the total amounts of glutamate determined in the *B. subtilis* cell pellet and in the supernatant.

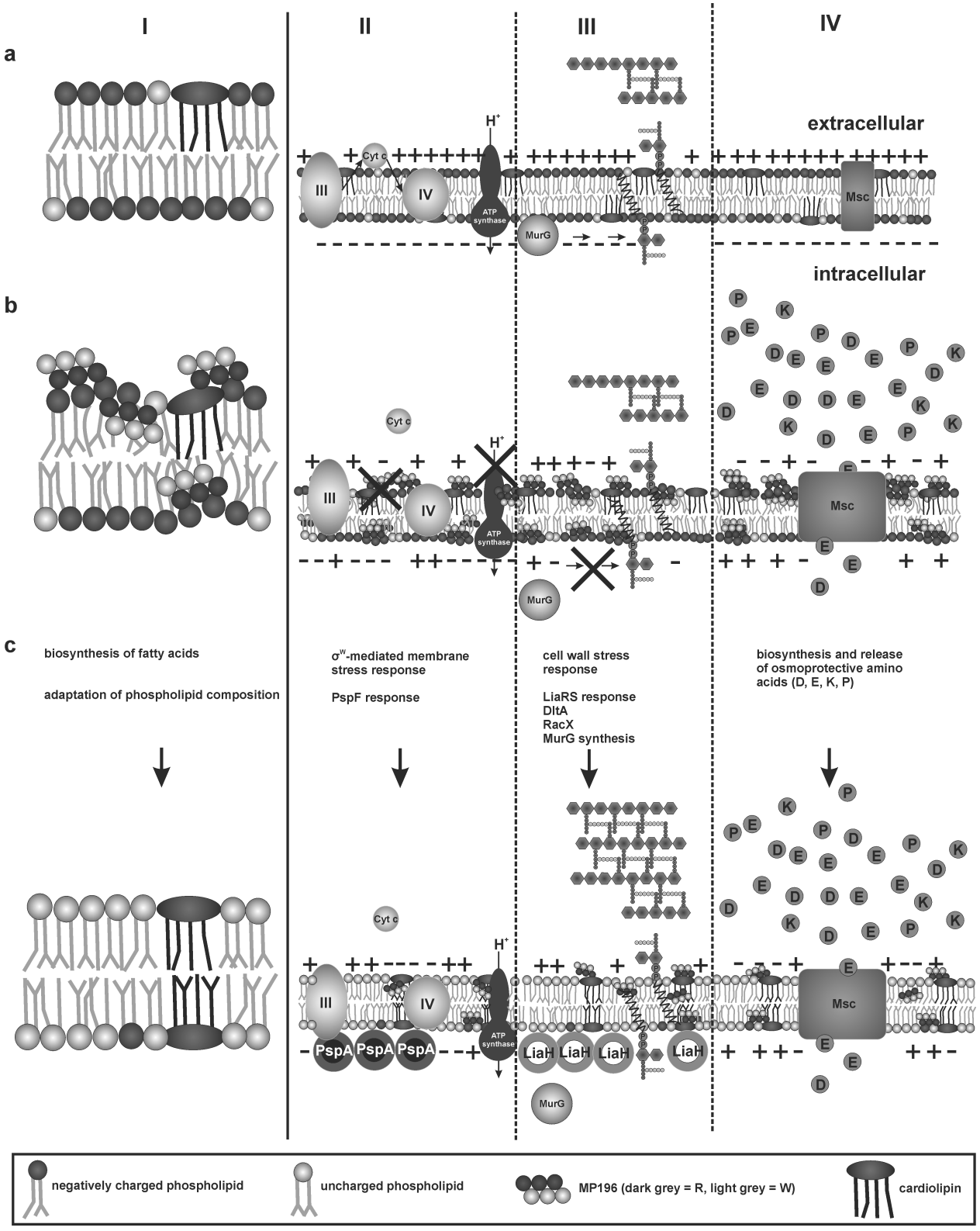
I
II
III
IV
a
b
c
extracellular
intracellular
Cyt c
H+
III
IV
ATP synthase
MurG
Msc
biosynthesis of fatty acids
adaptation of phospholipid composition
σW-mediated membrane stress response
PspF response
cell wall stress response
LiaRS response
DltA
RacX
MurG synthesis
biosynthesis and release of osmoprotective amino acids (D, E, K, P)
PspA
LiaH
negatively charged phospholipid
uncharged phospholipid
MP196 (dark grey = R, light grey = W)
cardiolipin

Figure S9: Model of the mechanism of action of MP196 and the bacterial response to exposure. Model of changes to membrane structure **(I)**. Membrane harboring the respiratory chain **(II)**, the cell wall biosynthesis machinery **(III)**, and mechanosensitive channels **(IV)**. **(a)** Intact *B. subtilis* membrane, **(b)** influence of MP196 on membrane architecture and membrane-associated components, **(c)** stress adaptation of *B. subtilis* to MP196-mediated membrane stress. Msc: mechanosensitive channel